PNNL-10997
UC-810
Project Technical Information

Final Technical Report: Effects of Water on Properties of the Simulated Nuclear Waste Glasses

H. Li
M. Tomozawa

February 1996

Prepared for the U.S. Department of Energy
under Contract DE-AC06-76RLO 1830

Pacific Northwest National Laboratory
Operated for the U.S. Department of Energy
by Battelle Memorial Institute

Battelle

PNNL-10997
UC-810
Project Technical Information

Final Technical Report: Effects of Water on Properties of the Simulated Nuclear Waste Glasses

H. Li
M. Tomozawa

February 1996

Prepared for
the U.S. Department of Energy
under Contract DE-AC06-76RLO 1830

Pacific Northwest National Laboratory
Richland, Washington 99352

DISCLAIMER

PACIFIC NORTHWEST NATIONAL LABORATORY
operated by
BATTELLE
for the
UNITED STATES DEPARTMENT OF ENERGY
under Contract DE-AC06-76RLO 1830

Printed in the United States of America

Available to DOE and DOE contractors from the Office of Scientific and Technical Information, P.O. Box 62, Oak Ridge, TN 37831; prices available from (615) 576-8401.

Available to the public from the National Technical Information Service, U.S. Department of Commerce, 5285 Port Royal Rd., Springfield, VA 22161


The document was printed on recycled paper.

Final Technical Report

Effects of Water on Properties of the Simulated Nuclear Waste Glasses

(May 1, 1993 - May 12, 1994)

to

Battelle Pacific Northwest Laboratories
Richland, Washington 99352

by

Hong Li and Minoru Tomozawa

Materials Engineering Department
Rensselaer Polytechnic Institute
Troy, New York 12180-3950

1. Introduction

For isolation of nuclear wastes through the vitrification process, waste slurry is mixed with borosilicate based glass and remelted at high temperature. During these processes, water can enter into the final waste glass. It is known that water in silica and silicate glasses changes various glass properties, such as chemical durability, viscosity and electrical conductivity. These properties are very important for processing and assuring the quality and safety controls of the waste glasses. The objective of this project was to investigate the effect of water in the simulated nuclear waste glasses on various glass properties, including chemical durability, glass transition temperature, liquidus temperature, viscosity and electrical conductivity. This report summarizes the results of this investigation conducted at Rensselaer during the past one year.

2. Experimental Procedures

2.1 Preparation of Glasses with Different Water Contents

Three types of the simulated nuclear waste glasses, CVS2-18, CVS2-52 and CVS2-74, were provided by Battelle Pacific Northwest Laboratories (Richland, WA) for this project. Table I summarizes the chemical compositions of these glasses. The water concentration in these glasses was altered by remelting under different water vapor pressure and, subsequently, the hydroxyl concentration was determined by IR spectroscopy.

2.1.1 Glass Melting under Water Vapor

Three as-received glasses were crushed and remelted at 1150±4 °C in an 80 ml Pt crucible using a CM rapid temperature furnace (CM Furnace Inc., N.J.). The furnace temperature was controlled by a Eurotherm microprocessor-based temperature controller and monitored by a type S thermocouple. For the preparation of the glasses with different water concentrations, glass melts were exposed to water vapors corresponding to a saturated vapor pressure of water at various temperatures: 50 °C (93 mmHg), 80 °C (355 mmHg) and 100 °C (760 mmHg) [2]. The water vapor was generated from a deionized water reservoir kept in a temperature-controlled hot water bath. To ensure the homogeneous distribution of water in the glass melt, water vapor was bubbled through the melt at the flow rate of 68.5 ml/min. For the case of 760 mmHg water vapor, the air flow rate was reduced to 32.9 ml/min to prevent the melt from splashing out of the Pt crucible. The flow rate was controlled by a Manostat flowmeter,

Figure 1 shows a schematic diagram of the experimental setup for the glass melting. Heating tape was used to keep the vapor inlet above 100 °C so that no water vapor condensation would take place there. The distance D1, between the bottem of the crucible and the tip of the lifted Pt-tube is about 50 mm and the distance D2, between the bottom of the crucibe and the tip of the immersed Pt-tube is about 5 mm as shown in Figure 1.

The melting furnace was preheated to 1150 °C in air. The Pt crucible, containing about 80 g of crushed as-received glass, was then inserted into the furnace. For the first 15 min, the water vapor was passed on to the top of the glass melt through the Pt-tube kept at the distance D1 from the bottom of the crucible, as shown in Figure 1. The tube was then inserted into the melt to the distance D2 from the crucible bottom, introducing water vapor directly into the melt for 30 min. Then, the Pt tube was pulled out of the melt to the distance D1 and the melt was fined at this temperature for additional 20 min, while the water vapor was still passed on to the top of the melt. The total melting time was 65 min.

Once the remelting procedures were completed, the melt was poured into a copper mold with approximate dimension of 50 mm x 50 mm x 8 mm and then immediately transfered to an annealing furnce. The glass plates were kept at 400 °C for 30 min and then furnace cooled to room temperature.

2.1.2 Quantification of Water in Glasses

2.1.2a Hydroxyl Absorption Coefficient Determined by IR Spectroscopy

Specimens of 15 mm x 15 mm x 0.6 mm were cut from the annealed glass samples. Both faces of the specimens were polished using 320, 400 and 600 grit SiC papers and

finally with CeO_2 slurry. After polishing, the specimens were cleaned with ethanol in an ultrasonic cleaner twice for a total of 4 min, each time using fresh ethanol.

The relative hydroxyl concentration in the glasses was determined by IR absorbance at the wavenumber ~3550 cm^{-1} [3-5]. An example of the data is shown in Figure 2. The hydroxyl absorption peak intensity as a function of specimen thickness was measured using a Perkin-Elmer 1800 FTIR (Perkin-Elmer Corp., KY) to confirm the applicability of Beer's law to the colored specimens of the present glasses. According to Beer's law:

$$A = \log (I_o/I) = \varepsilon C d \qquad (1)$$

where

A: hydroxyl absorbance at ~ 3550 cm^{-1}

I_o, I: incident and transmitted IR intensities at ~ 3550 cm^{-1}, respectively after reflection correction

ε: extinction coefficient (mol/*l*-cm)

C: hydroxyl concentration (mol/*l*)

d: specimen thickness (cm)

Specimen thickness, d, was reduced successively by mechanical polishing and the hydroxyl absorbance, A, was determined after each successive reduction of specimen thickness.

At wavenumber ~ 2700 cm^{-1}, a second absorption peak was apparent for all three glasses as shown in Figure 2. This peak is an overtone of the B-O fundamental stretching band [6,7].

2.1.2b Hydroxyl Extinction Coefficient Determined by IR Spectroscopy and Weight Loss Method

To determine the hydroxyl concentration from IR absorbance, the extinction coefficient, ε, has to be known. The weight loss method was used to determine the extinction coefficient for these glasses. According to Pearson et al. [8], during the dehydration of glass specimen, hydroxyl in the specimen decreases according to:

$$2OH_{glass} \text{------>} H_2O_{gas} + O_{glass} \qquad (2)$$

and the decrease of OH causes the specimen weight loss and the reduction in the intensity of IR hydroxyl absorption. The extinction coefficient, ε_{OH} (lit/mol-cm) or ε'_{OH} (1/cm-ppm), of the IR hydroxyl absorption is determined by [8]:

$$\varepsilon_{OH} = 10^{-3} (M_{H2O} / 2M_{OH}) (W / d) (\Delta A / \Delta W) (M_{OH} / D_{glass}) \qquad (3a)$$

or

$$\varepsilon'_{OH} = 10^{-6} (M_{H2O} / 2M_{OH}) (W / d) (\Delta A / \Delta W) \qquad (3b)$$

where ($M_{H2O}/2M_{OH}$ = 18/34) refers to the formation of one mole of H_2O by the destruction of two moles of OH, (W/d) is the ratio of the initial specimen weight to the specimen thickness, ($\Delta A/\Delta W$) is the ratio of the change of IR hydroxyl absorption to the change of the weight of specimen, and (M_{OH}/D_{glass}) is the ratio of the molar weight of hydroxyl to the density of the glass.

Specimens of about 15 mm x 15 mm x 0.3 mm were cut from the annealed as-received CVS2-18, 52 and 74 glasses. Both faces of the specimens were polished using 320, 400 and 600 grit SiC papers and finally with CeO_2 slurry. After polishing, the specimens were cleaned with ethanol in an ultrasonic cleaner twice for a total of 4 min, each time using fresh ethanol.

To determine the ratio of ($\Delta A/\Delta W$), each specimen was dehydrated at 450 °C in a dry nitrogen atmosphere. The sample was periodically taken out of the furnace to measure both its weight using a precession balance Mettler AE163, with a resolution of $\pm$0.01 mg, and the IR spectrum using the IR spectrophotometer.

The density of the as-received and remelted glasses were determined by the Archimedean method using deionized water at room temperature. Specimens were cut in dimensions about 2 cm x 1.5 cm x 1 cm from the remelted/annealed glasses with different water concentrations. Then, the specimens were washed with ethanol in an ultrasonic cleaner three times, changing the liquid each time for a total of 6 min. A precision balance Mettler H80, with a resolution of $\pm$0.1 mg, (Mettler Instrument Corp., NJ) was used for the weight measurement. Four specimens were measured for each glass having the same water concentration and the average value and one standard deviation were calculated. The density was determined as:

$$D = M_S / V_S = D_{H2O}(M_{ds} - M_{dc}) / [(M_{ds} - M_{ws}) - (M_{dc} - M_{wc})] \qquad (4)$$

where

M_S : weight of specimen (g)

V_S : volume of specimen (cm^3)

M_{ds}: weight of specimen and sample container in dry condition (g)

M_{dc}: weight of sample container in dry condition (g)

M_{ws}: weight of specimen and sample container in wet condition, immersed in water (g)

M_{wc}: weight of sample container in wet condition, immersed in water (g)

D_{H2O}: density of pure water at room temperature, 1.0 g/cm^3

2.1.2c Water Concentration in Glass

Knowing the hydroxyl absorption coefficients, (absorbance, A, divided by specimen thickness, d), and the hydroxyl extinction coefficient, ε_{OH} or ε'_{OH}, the concentrations of water in hydroxyl form contained in these glasses were calculated using Eqaution (1).

2.2 Chemical Durability

The chemical durability of the simulated nuclear waste glasses was evaluated using both the MCC-1 and PCT methods in terms of the normalized elemental mass loss of silicon, boron, lithium and sodium.

2.2.1 MCC-1 Chemical Durability Test

2.2.1a Specimen Preparation

Specimens were cut in dimensions of 15 mm x 15 mm x 0.5 mm using a diamond saw. For all specimens, the cutting speed was fixed and water was used as cooling liquid. After cutting, the specimens were cleaned in fresh ethanol three times (3 min each) in an ultrasonic cleaner. Weight of the specimen was measured using the precision balance Mettler H80. The specimen dimensions were measured under 10x magnification using an optical microscope equipped with a digital micrometer, from which the total surface area of each specimen, SA, was determined.

2.2.1b MCC-1 Test Procedure

The MCC-1 test was used to evaluate the chemical durability of these simulated nuclear waste glasses. The test matrix is given in Table II. Each specimen was separately placed in an individual Teflon PFA leach container and submerged in water. ASTM type I water was used, which was deionized and distilled with an electrical resistance of 18 megohm (SPEX Industries, Inc., NJ). The leach containers were cleaned according to the MCC-1 method [9]. The ratio of the specimen surface area to the volume of water, (SA/V), was fixed at 10 m^{-1} following the MCC-1 procedure [9].

Prior to the MCC-1 test, the initial weight of (specimen+water+leach container) was recorded. The initial pH value of ASTM type I water in the leach container was also measured using a 701A digital pH/mV meter (Orion Research Inc., MA) precalibrated using reference buffer solutions (Fisher Scientific, NY).

All specimens were put into the Fisher ISOTEMP-300 oven preset at 90 °C. The total test duration was 28 days, during which the furnace temperature was kept at 90±0.5 °C, monitored by using a type S thermocouple. After the MCC-1 test, the leach containers were removed from the oven and cooled to room temperature. Then the weight of

(specimen+water+container) and the final pH value of leachate were remeasured. After cleaning with fresh ethanol using an ultrasonic cleaner and drying in air, all specimens were weighed.

2.2.1c Determination of Normalized Elemental Mass Loss

The concentrations of four elements, silicon, boron, lithium and sodium, in the leachate were analyzed. Prior to the measurement, all leachates were filtered through 0.45 μm membrane according to the MCC-1 method [9]. DC plasma emission spectroscopy was applied to determine each element concentration, using a Beckman Spectran V emission spectrometer (Beckman Instruments, Inc., CA). To establish a calibration curve for each element, solutions of that element with known concentration were prepared using a standard reference solution (SPEX Industries, Inc., NJ). Figure 3 illustrates the calibration curves for the four elements (Si, B, Li and Na). The value in a parenthesis is the wavelength for that particular element. These lines were selected with the consideration of their linear dynamic ranges [10], detection limits [10] and small signal from background (mainly water). The following calibrated lines, determined by the linear regression best fit, were used to determine the concentration of each element in the leachate:

Silicon:	$Si \text{ (ppm by wt)} = (I_{Si} - 146.806) / 13.656$	(6a)
Boron:	$B \text{ (ppm by wt)} = (I_{B} - 144.547) / 14.163$	(6b)
Lithium:	$Li \text{ (ppm by wt)} = (I_{Li} - 64.644) / 22.519$	(6c)
Sodium:	$Na \text{ (ppm by wt)} = (I_{Na} - 170.155) / 298.446$	(6d)

where I is the intensity of the spectral line (D.C. mA). The linear regression coefficients, r^2, for these four lines shown in Figure 3 are greater than 0.999.

According to the MCC-1 method [9], the dissolved element concentration is expressed in terms of the normalized elemental mass loss, $(NL)_i$:

$$(NL)_i = C_i / f_i \, (SA/V) \qquad (g/m^2) \qquad (7)$$

where C_i = concentration of element i in the 0.45 μm filtered leachate (g/m^3)

f_i = mass fraction of element i in the unleached specimen

SA/V = ratio of specimen surface area to volume of leachant (m^{-1})

In Equation (7), f_i values were determined from the compositions of each as-received glass. Table III lists the selective chemical compositions and the related f_i-value of Si, B, Li and Na for the three glasses investigated.

2.2.2 PCT Chemical Durability

2.2.2a Sample Preparation

Samples were prepared by crushing glass into powder using an alumina motar and pestle. The powder size ranged from 75 to 150 μm and was selected by using 100 and 200 mesh sieves. To remove the fines, prepared powder was washed twice using fresh ethanol in an ultrasonic cleaner. Then the powder was dryed at room temperature overnight.

2.2.2b PCT Procedure

Dry powder sample was weighed using the precision balance Mettler H80. ASTM type I water (deionized water, electrical resistance of 18 megohm, SPEX Industries, Inc., NJ) was then mixed with the powder in the ratio of 10 ml of water per gram of powder [11]. The total volume of water used for each sample was determined using the Mettler H80 balance. Assuming a cubic shape for a particle, the mixture of powder and water had a surface area of sample to the volume of water ratio, (SA/V), of ~2000 m^{-1}.

Table IV shows the test matrix. Powder samples were placed, submerged in water, in a Teflon PFA leach container. The leach containers were cleaned according to the procedures described in the MCC-1 method [9].

Prior to the PCT, the initial weights of (sample+water+leach container) were recorded. The initial pH values of both blank water and solutions of (powder+water) in leach containers were measured at room temperature using the 701A digital pH/mV meter pre-calibrated using the reference buffer solutions.

All samples were placed in a Fisher ISOTEMP-300 oven preset at 90 °C. The total test duration was 7 days, during which time the furnace temperature was kept at 90±0.5 °C, monitored with a type S thermocouple. After the PCT, all leach containers were removed from the furnace and cooled in air overnight. Then the weight of (sample+water+container) and the final pH value of the leachate were remeasured.

2.2.2c Determination of Normalized Elemental Mass Loss

The determination of the elemental concentration for silicon, boron, lithium and sodium in the leachate followed the same procedures described previously (cf. 2.2.1c). The DC plasma emission spectroscometer was recalibrated using standard reference solutions of silicon, boron, lithium and boron. Since the concentration of sodium in the PCT leachate was much higher than that in the MCC-1 leachate, a different wavelength for sodium was used to ensure the concentration falling in the linear dynamic range of the sodium spectrum.

Figure 4 shows the calibration curves for the elements involved. The value in parentheses is the wavelength for that particular element. The following calibrated lines,

determined by the linear regression best fit, were used to determine the concentration of each element in the leachate:

Silicon:	Si (ppm by wt) = (I_{Si} – 168.194) / 13.604	(8a)
Boron:	B (ppm by wt) = (I_B – 137.898) / 14.065	(8b)
Lithium:	Li (ppm by wt) = (I_{Li} – 79.518) / 22.730	(8c)
Sodium:	Na (ppm by wt) = (I_{Na} – 133.416) / 9.764	(8d)

where I is the intensity of the spectral line (D.C. mA). The linear regression coefficients, r^2, for these four lines shown in Figure 4 are all greater than 0.999. Comparing Equations 8(a-c) with Equations 6(a-c), a good agreement between the two sets of calibrations was found.

The chemical durability was evaluated in terms of the normalized elemental mass loss, $(NL)_i$, defined by Equation (7).

2.3 DSC Glass Transition Temperature

The glass transition temperature, T_g , was measured by the differential scanning calorimetry (DSC) method for three types of glasses with different water contents. A Perkin-Elmer DSC-4 (Perkin-Elmer Corp., KY) was used and the instrument was calibrated using indium metal. The sample was in powder form with particle size about 280 μm and was mechanically sealed in a gold pan. Since the glass transition temperature depends on the heating and cooling rates [12], the sample was cooled from 520 °C to 420 °C at a cooling rate of 2.5 °C/min. The heating rate during the DSC scan was 10 °C/min for all measurements. Figure 5 represents the DSC scan of NBS standard SRM711 glass. The DSC glass transition temperature, T_g, was determined by the conventional manner as shown.

2.4 Liquidus Temperature

2.4.1 Sample Preparation

The liquidus temperature was determined for both as-received and re-melted glasses. Samples were prepared by crushing glass into small pieces which were preheat-treated in a Pt-5%Au combustion boat (110 mm x 8 mm x 10 mm) at 690 °C for 24 hr. The as-received glass was heat-treated in air and the glass remelted at 1150 °C under 355 mmHg water vapor pressure was heat-treated in 355 mmHg water vapor.

2.4.2 Liquidus Temperature Measurement

After the pre-heat-treatment, the sample with the combustion boat was heat-treated in a Lindberg SIB 3-Zone gradient furnace (Lindberg SIB Division of Sola Basic Ind., Watertwon, WI) for 24 hr in air or 355 mmHg water vapor. The temperature profile of the furnace was calibrated using a type K thermocouple. As shown in Figures 6(A-B) for two different temperature distributions, the temperature calibration curves were established by using the 6th order polynomial best fit:

$$T\ (^{o}C) = a_o + a_1X + a_2X^2 + a_3X^3 + a_4X^4 + a_5X^5 + a_6X^6 \qquad (9)$$

where X is the distance from a fixed reference position in the furnace and values of the coefficients, a_i, are as shown in Figures 6(A, B). The regression correlation coefficients for the profiles were greater than 0.999.

After the heat-treatment in the gradient furnace, each sample was removed from the lower temperature end of the furnace and then placed in an annealing furnace preset at 520 °C for 2 hr and then furnace cooled to room temperature. To determine the liquidus temperature, a long thin plate was sliced from the middle of the annealed sample bar. The sample plate was then cut into several pieces and mechanically polished using 240, 320, 400 and 600 grit SiC abrasives and finally with 1 μm CeO_2 slurry. The polished specimens had a thickness of ~ 450 μm. Each thin piece was scanned using a Philips 5520 X-ray diffractometer (Philips Electronic Instruements Co., NY) operated at 40 kV-35 mA using Cu $K_{\alpha 1}$ and $K_{\alpha 2}$ radiation. The liquidus temperature was determined as the highest temperture at which the sliced piece showed no crystalline peak at a 2θ angle of ~ 30°, which is the most intense and stable diffraction peak observed for all specimens.

2.5 Viscosity of Glass Melts

The viscosity of the glass melt was measured in the temperature range of 950 °C to 1250 °C at 50 °C intervals in ambient air, 93 mmHg, 355 mmHg and 760 mmHg water vapor atmosphere corresponding to the atmosphere of each sample preparation (cf. 2.1.1). The viscosity apparatus consisted of a CM 1300 tube furnace (CM Furnace Inc., NJ) and a Brookfield LVT viscometer (Brookfield Engineering Inc., MA). A Pt-20%Rh disk type spindle (0.5" diameter x 0.08" thickness) was used for the viscosity measurement, as shown in Figure 7. The temperature of the furnace was monitored by a type S thermocouple and controlled within ± 1 °C during the measurment.

The viscosity, η (Pa.s), of the glass melt was determined [13] according to:

$$\eta = K \text{ (Reading, unitless)} / \text{(Spindle Rotation Speed, rpm)} \qquad (10)$$

where K is the cell constant (Pa.s-rpm) for a given condition and is influenced by the crucible dimension, volume of melt and the spindle geometry. In this study, a cylindrical Pt crucible with 50 ml volume was used and the volume of glass melt used was about 40 ml. The spindle immersion depth into the glass melt was fixed at 0.9", which was controlled by using a micrometer.

To determine the cell constant, K, Brookfield standard oils (Brookfield Engineering Inc., MA) with known viscosity values, 12.2 Pa.s and 103.5 Pa.s, were used. These viscosity values are close to those of the glass melts in the temperature range of the measurement. The cell constant was determined by the slope of the best fit line shown in Figures 8 (A, B). For the immersion depth of 0.9", the K value was determined to be 1.406 ± 0.018 Pa.s-rpm.

2.6 Electrical Conductivity

The elctrical conductivity, using the AC method, of the glass melt was measured in the temperature range of 950 °C to 1250 °C at 50 °C interval in ambient air, 93 mmHg, 355 mmHg and 760 mmHg water vapor atmosphere corresponding to the atmosphere of each sample preparation (cf. 2.2.1). The conductivity apparatus consisted of the CM 1300 tube furnace and a 1689 GenRad RLC digibridge (QuadTech, Inc., MA). Pt wire was used as the electrode. The temperature of the furnace was monitored by a type S thermocouple and was controlled within ± 1 °C during the measurment.

The conductivity, σ (S/m), of the glass melts was determined using the method reported by Boulos, Smith and Moynihan [14] :

$$\sigma = Y/R \qquad (11)$$

where Y is the cell constant (m^{-1}) and R is the resistance (ohm). R was measured using the AC method in which a model of an equivalent paralell circuit (R_p, C_p) was used. The complex impedance, Z*, of the circuit is given by [15]:

$$Z^* = Z' - j\,Z'' \qquad (12)$$

where

$$Z' = G_p(\omega)/[G_p^2(\omega)+\omega^2C_p^2(\omega)] \qquad \text{(ohm)}$$
$$Z'' = \omega C_p(\omega)/[G_p^2(\omega)+\omega^2C_p^2(\omega)] \qquad \text{(ohm)}$$

and $G_p(\omega)$ is the conductance (1/ohm), $C_p(\omega)$ is the capacitance (Farad) and ω is the angular frequency (1/sec).

To determine the cell constant, Y, standard KCl aqueous solutions with concentrations of 0.1D (7.47896 g KCl per 1000 g water in air) and 1.0D (76.6276 g KCl per 1000 g water in air) were prepared using pure KCl powder and deionized and distilled water at room temperature following the method of Parker and Parker [16] (D is for demal, equal to equivalents per dm^3). The conductivity values, at 25 °C in air, were previously reported as 1.28524 S/m for 0.1D KCl and 11.1322 S/m for 1.0D KCl [16]. In this study, the AC frequency range for the measurment was from 1 kHz to 100 kHz. The immersion depth of the electrode was 0.7" controlled by a micrometer. The cylindrical Pt crucible with 50 ml volume was used and the volume of glass melt was about 40 ml. Figure 9 shows the Z'-Z" plot of KCl solutions. The resistance, R, for the solutions was determined from the intercept on the Z'-axis using the linear regression method. The cell constant, Y, was then calculated to be 67.60 ± 2.42 m^{-1} using Equation (11).

3. Results

3.1 Characterization of Water Content in Glass

3.1.1 Hydroxyl Absorption Coefficient

Figures 10(A-C) show the IR absorption of hydroxyl versus the specimen thickness for as-received glasses and glasses remelted at 1150 °C under various water vapor atmospheres. The linear relation indicates the applicability of Beer's law to the present specimens and the hydroxyl absorption coefficients, A/d or εC, were determined from the slopes of the lines and are summarized in Table V. The linear regression coefficients were greater than 0.98 in all cases. A good reproducibility of the hydroxyl content in the glass melt made by the current melting procedures was confirmed.

3.1.2 Hydroxyl Extinction Coefficient

Using the dehydration method, weight loss and IR hydroxyl absorbance decrease of the specimen were periodically measured. Figure 11 illustrates the change of the IR absorbance as a function of the specimen weight loss for CVS2-18, 52 and 74. In all cases,

a linear relationship between these two quantities exists. Linear regression analysis yields the best fit line for each glass, the slopes, ($\Delta A/\Delta W$), of which are summarized in Table VI.

The densities for CVS2-18, 52 and 74 glasses are also summairzed in Table VI. It appears that the density is the same for most glasses within the error range of the method used. No effect of water on the density could be detected. Slightly lower density values were noticed for as-received CVS2-18 and CVS2-74, which probably resulted from the presence of the bubbles in these specimens.

Using Equation 3(a-b), the extinction coefficients, ε_{OH} and ε'_{OH}, were calculated and are listed in Table VI. The resulting hydroxyl extinction coefficients, ε_{OH}, were found to be smaller than the previously published data: 30±5 *l*/mol-cm for sodium borosilicate glass, 27.5 *l*/mol-cm for Corning 7740 and 28 *l*/mol-cm for Corning 7251[8]. The difference is probably related to differences in the glass compositions.

3.1.3 Water Concentration in Glass

Knowing the extinction coefficient and the hydroxyl absorption coefficients, (absorbance/specimen thickness), the hydroxyl concentration in these glasses were calculated according to the Beer's law:

$$A_{OH} = \varepsilon_{OH} C_{OH} d \qquad (13a)$$

or

$$A_{OH} = \varepsilon'_{OH} C'_{OH} d \qquad (13b)$$

where C_{OH} and C'_{OH} are the concentration of hydroxyl in the specimen with the units of (mol/liter) and (ppm by wt), respectively, and d is the specimen thickness (cm). It is more convenient to express the hydroxyl concentration in the latter units of ppm by weight. Table VII summarizes the hydroxyl concentrations for the prepared glass samples. The results show that under the same melting condition, CVS2-18 has the highest hydroxyl concentration, while CVS2-74 has the lowest.

The dependence of water concentration in glass on the water vapor pressure is shown in Figure 12. The data indicate that, at relatively low water vapor pressures, the hydroxyl concentration is a linear function of the square root of water vapor pressure, $\sqrt{p_{H2O}}$, as expected [3, 17]. The concentraton, however, deviated from linearity under the higher water vapor pressure of 760 mmHg. This may be related to the volatilization of some glass elements during the glass melting under high water vapor presence. It is known that water promotes the volatilization of sodium and boron [18].

3.2 Chemical Durability

3.2.1 MCC-1

The signal intensity from the DC plasma emission spectrometer of the element i, I_i, in the leachate was recorded automatically. Applying Equations 6(a-d), the concentrations of Si, B, Li and Na were determined for each leachate and are tabulated in Appendix A1. The normalized elemental mass loss, $(NL)_i$, was computed according to Equation (7). Figures 13(A-C) illustrate the average elemental mass losses of Si, B, Li and Na versus the hydroxyl concentration (cf. Table VII) for CVS2-18, 52 and 74, respectively. The $(NL)_i$ values are tabulated in Appedix A2.

For a given glass, Figures 13(A-C) show that the normalized elemental mass loss, $(NL)_i$, has a general trend of $(NL)_{Si} < (NL)_B < (NL)_{Li} < (NL)_{Na}$. Among these three glasses, for the four elements, CVS2-18 has much higher $(NL)_i$ values than both CVS2-52 and CVS2-74. Comparing CVS2-52 with CVS2-74, the elemental mass losses of Si, B and Na were slightly higher for the former, while that of Li was about the same for both glasses. Results also indicated that the dissolution of each element was mainly influenced by the glass compositions and that the effect of hydroxyl concentration was rather small.

The change of pH in the leachate before and after the MCC-1test was monitored. Appendix A1.2 also summarizes average pH values with one standard deviation. The initial pH of type I water was 4.85 ± 0.08. After the MCC-1 test of the simulated nuclear waste glasses, pH was increased to approximately 9.00, while a blank water after the test was only pH 5.39. Hence, the increase in pH of the leachate after 28 days was associated with the glass leaching. Two exceptional cases were found for the as-received CVS2-74. Two out of three samples tested after 28 days showed pH 6.73 and pH 6.52, while the third sample leachate had a pH 8.97 which was at the same level as the rest of leachates. In these cases, the $(NL)_i$ values of all four elements investigated were also much lower. Therefore, for the as-received CVS2-74 glass, only one $(NL)_i$ datum is listed in Appendix A2 for each element.

During the MCC-1 test, the weight loss of the leachate due to water evaporation was found to be less than 5 wt%. The specimen weight before and after the test was also monitored. All specimens lost weight slightly as the result of the glass dissolution. Among the three glasses, CVS2-18 showed the greatest weight loss, 9.4 ± 0.6 g/m^2, as compared with 5.5 ± 0.6 g/m^2 for CVS2-52 and 6.6 ± 0.7 g/m^2 for CVS2-74.

3.2.2 PCT

The signal intensity from the DC plasma emission spectrometer of the element i, I_i, in the leachate was meaured three times. The average intensity value and one standard

deviation from the three measurements were used for the determination of the concentrations for Si, B, Li and Na using Equations 8(a-d). The results are tabulated in Appendix B1. Figures 14(A-C) illustrate the elemental mass losses of Si, B, Li and Na versus the hydroxyl concentration. The data are tabulated in Appendix B2. The results show that samples having higher hydroxyl concentration exhibit a higher amount of dissolution.

For a given glass, Figures 14(A-C) show that the normalized elemental mass loss, $(NL)_i$, has a general trend of $(NL)_{Si} < (NL)_{Na} < (NL)_B < (NL)_{Li}$. Among these three glasses, for all four elements, CVS2-18 has the highest $(NL)_i$ values, while CVS2-74 has the lowest ones. Results in Appendix B2 indicate that for the long-term chemical durability of the glasses tested in water, the dissolution of each element was mainly influenced by the glass chemical compositions. However, for a given glass, the effect of hydroxyl concentration on the dissolution was also evident. Boron is a good indicator of the chemical durability. Figure 15 shows that the $(NL)_B$ increases with the hydroxyl concentration in glass for all three glasses and the results can be fitted using a linear relationship. The slopes of the best fit lines with the linear regression coefficients are summarized in Table VIII.

pH of a blank water was 4.94 at room tempearture prior to the PCT. Right after mixing the powder with water at room temperature, pH of the leachate increased significantly with respect to that of a blank water. Appendix B3 surmarizes the pH values right after mixing the powder with water for all sample leachates. The final pH values were remeasured at room temperature after the PCT, and are also listed in Appendix B3. Final pH of the blank water was 5.48. Among these three glasses, pH values for CVS2-18 were the highest, while those of CVS2-52 were the lowest. The weight loss of the leachants during the PCT measurement was less than 1.0 wt%.

3.3 DSC Glass Transition Temperature

Figures 16(A-D) illustrate the DSC scans for CVS2-18 with four different water concentrations. Similar scans are shown in Figures 17(A-D) and Figures 18(A-D) for CVS2-52 and CVS2-74, respectively. Table IX summarizes DSC glass transition temperatures, T_g, for these glasses. Except for the as-received glasses, the results show that T_g decreases with increasing water concentration in the samples for CVS2-18 and CVS2-74. The effect of water on the change of T_g, however, was rather small for CVS2-52.

It was noted that there was a lack of a consistent trend for the as-received glasses, for which the lower DSC transition temperatures could not be obtained inspite of their

higher hydroxyl concentrations. These as-received glasses have different thermal histories and possibly a slightly different glass composition from those remelted in our laboratory.

3.4 Liquidus Temperature

Figures 19(A-C) show X-ray diffraction patterns of powders prepared by grinding the three as-received glasses after the heat-treatment in ambient air at 690 °C for 24 hr. It appears that amount of crystallization is the highest for CVS2-52 and the lowest for CVS2-74. Table X summarizes the liquidus temperature, T_L, for the as-received glasses: 842 °C for CVS2-18, 923 °C for CVS2-52 and 852 °C for CVS2-74. The uncertainty for the liqudus temperature was estimated to be -2 °C since the sample at 2 °C below the estimated liquidus temperature exhibited a very small X-ray diffraction peak at a 2θ angle ~30°.

Figures 20(A-C) show X-ray powder diffraction patterns, after heat-treatment at 690 °C in 355 mmHg water vapor for 24 hr, for the three glasses which had been remelted at 1150 °C under 355 mmHg water vapor. From the comparison of Figures 20(A-C) and Figures 19(A-C), it appears that the wet atmosphere promoted the devitrification for all glasses. Table X also summaries the liquidus temperatures for the remelted glasses heated in 355 mmHg water vapor for 24 hr after crystallization at 690 °C for 24 hr. It was found that the liquidus temperature increased by about 25 °C: 871 °C for CVS2-18, 946 °C for CVS2-52 and 872 °C for CVS2-74. The uncertainty of the liquidus temperature was -5 °C for CVS2-18, -6 °C for CVS2-52 and -16 °C for CVS2-74. The higher uncertaintly resulted because the samples were heat-treated in a higher temperature gradient.

3.5 Viscosity

Figures 21(A-C) show the logarithmic viscosity as a function of temperature for theses glasses remelted under different atmospheres. The viscosity data are tabulated in Appendix C1. In general, CVS2-52 had slightly higher viscosities throughout the temperature range than those of CVS2-18 and CVS2-74. For a given glass and at a specific temperature, an expected trend of lower viscosity with increasing water content was not obtained, within the experimental error. This can be seen in Figures 22(A-C) which represent the viscosities of the glass melts at 1150 °C against the water concentrartions in these glasses (c.f. Table VII).

3.6 Electrical Conductivity

Appendix D1 summarizes the conductivity data for all glasses under different atmospheres. Figures 23(A-C) illustrate logarithmic resistivity as a function of temperature

for the ease of comparison with the viscosity data. In general, CVS2-18 has slightly higher resistivities throughout the temperature range employed. Figures 24(A-C) represent the electrical conductivity versus the water concentrations in the glasses at 1150 °C. The electrical conductivity of these glasses appears to exibit a minimum when plotted against the water contents (c.f. Table VII), except for CVS2-74.

4. Discussions

4.1 Water Content

Water content in the glasses was determined by IR spectroscopy. In this method, the water content is influenced by the extinction coefficient, which was determined by the dehydration-weight loss method. It was assumed that the only source of weight change during the dehydration treatement is the loss of water (c.f. Equation (2)). Since the simulated nuclear waste glasses contain transition metal ions which can change their oxidation state easily, a portion of the weight change might come from the change of the oxidation state, e.g.:

$$2OH_{glass} + Fe^{2+}{}_{glass} \text{ -------> } Fe^{3+}{}_{glass} + 2O_{glass} + H_2 \qquad (14)$$

This could cause an error in the extinction ceofficient and the absolute quantity of water. For a given glass, however, relative water content remains unaffected by the magnitude of the extinction coefficient.

4.2 Chemical Durability

The effect of water content on the dissolution rate was observed in the PCT method, namely, higher water content in the glass resulted in higher dissolution rates of Si, B, Li and Na. However, the influence of water on the leaching behavior was not detected in the MCC-1 method. Major differences between the two methods are that (i) the (SA/V) value is much higher for the PCT and (ii) the test duration is, however, shorter for the PCT. It is known that the chemical reaction of glass in water proceeds through the processes of (i) ion-exchange between the alkali ions of glasses and hydrogen (or hydronium ions) in water and (ii) breakdown of the glass network. A higher surface area to the volume of leachant provides more reaction sites for these processes. Hence it is considered that the difference in the (SA/V) value influences the glass dissolution process significantly.

Figure 25 illustrates the pH values before and after the two chemical durability tests, the PCT and the MCC-1. It is evident that for the PCT, the initial pH of the leachate, right after the powder was mixed with water at room temperature, was significantly higher than the initial value of leachate for the MCC-1. This is direct evidence for the fast ion-exchange taking place between the alkali and hydrogen (or hydronium) ions. The process can be expressed as [19]:

$$\equiv Si-OM + H_2O \text{ ------> } \equiv Si-OH + M^+ + OH^- \qquad (15)$$

where M^+ is the alkali ion. Also, as clearly shown in Figure 25, the final pH increased close to pH 10 after 7 days for the PCT, while in MCC-1 pH increased to ~9.0 after 28 days. Other previously reported data of the PCT and the MCC-1 demonstrated that there exists an initial sharp arise in pH level for the PCT which then stablizes at a slightly higher level, while for the MCC-1, the pH level increases gradually with time [20,21]. This is schematically represented in Figure 26.

Leaching of glass constituents into water involves not only the ion-exchange of alkali ions with hydrogen (or hydronium) ions as described by Eqaution (15), but also the breakdown and subsequent dissolution of the hydrolyzed glass network into the water. The process can be summarized as (i) free hydroxyl formed by reaction (15) attacking siloxane bonds at the leachate/glass interface [19]:

$$\equiv Si-O-Si\equiv + OH^- \text{ ------> } \equiv Si-OH + \equiv Si-O^- \qquad (16)$$

and (ii) dissolution of the leached layer via the reaction of nonbridging oxygen (NBO), $\equiv Si-O^-$ according to [19]:

$$\equiv Si-O^- + H_2O \text{ ------> } \equiv Si-OH + HO^- \qquad (17)$$

However, reactions (16) and (17) are very slow when pH of the leachate is low in the buffered solutions. Numerous studies on the dissolution of silica showed that the dissolution rate of silica in buffered solutions is not pH-dependent below pH8.5-9.0. Above pH ~8.5, the dissolution rate increases with the pH significantly.

Figures 27(A, B) sechmatically illustrate the concentration profile of alkali elements in the leached layer and the bulk for both the PCT and the MCC-1. Comparing the initial value of pH 8.6 for the PCT with that of pH 4.9 for the MCC-1, it is reasonable to assume that for the PCT measurement, dissolution of the glass network dominates during the most

of the test duration after the short, initial ion-exchange stage. For the MCC-1 measurement, on the other hand, the pH level of the leachate is low and the leaching process is expected to be dominated by the ion-exchange during the most of the test duration as shown in Figure 27(A). These hypotheses were further surported by the experimental results showing that the concentrations of silicon and boron were significantly higher after the PCT than those of silicon and boron after the MCC-1 (cf. Appendix B1 and A1).

Water in the glass creates NBO, making glass weaker and the dissolution rate higher. Although the inital ion-exchange could produce a much higher water concentration than the initial water concentration in the leachated layer, the time span for this stage would be very short before the network dissolution started to take over in the PCT. Furthermore, high pH values above 8.6 promotes the network dissolution. Thus the surface layer produced by ion-exchange can be quickly dissolved by the resulting high pH solution and the leaching process is dominated by the glass network disssolution in the PCT. It is expected therefore that the chemical durability of glass having higher water content would be poorer in the PCT.

On the other hand, in the MCC-1, the pH level is lower and the network dissolution is negligibly small. In this case, a leached layer forms, due to prolonged ion-exchange processes at low pH, and this layer contains higher water concentration than that in the bulk. Figure 28 shows the IR spectra of a CVS2-18 monolith sample before and after the MCC-1 test plus spectra after dehydration at 300 °C in ambient air for 1 and 16 hr. An increase in the amount of water is evident after the MCC-1 test. The dehydration spectra indicate that two types of water form in the glass by ion-exchange, strongly and lossely bonded hydroxyls. It has been reported that the thickness of hydration or ion-exchange affected layer is about 2 μm or less for the simulated nuclear waste glasses after the MCC-1 test [21]. Hence, the water concentration in the leachated layer can be more than 2 orders of magnitude higher than those of both as-received and remelted CVS2-18 glasses. Similar situations also exist for CVS2-52 and CVS2-74 glasses. Since the dissolution proceeds from the leachate/glass interface, the existance of a significantly higher water concentration in the leached layer should overide the effect of the preexisitng water in the glass, even when the network dissolution, rather than ion-exchange, is the rate controlling process. No detectable effect of the preexisting water content in glass on its chemical durability is, hence, expected in the MCC-1.

4.3 DSC Glass Transition Tempearture

The effect of water in glass on the glass transition temperature was observed. Glass having higher water content showed a lower transition temperature. This is consistent with previously reported data on various types of glasses [3,23].

4.4 Liqudus Temperature

For as-received glasses, the measured liquidus temperatures in ambient air have been previously reported: 865 °C for CVS2-18 and 850 °C CVS2-74 [24]. A good agreement was found between those obtained in this study and these values. In addtion, we observed that the liquidus temperature for the glass treated in wet atmosphere, 355 mmHg water vapor increased slightly, approximately 20 °C. Comparing x-ray diffraction patterns between samples heat-treated in ambient air and in the wet air, as shown in Figures 19(A-C) and Figures 20(A-C), the amount of crystalline phases increases by the wet treatment at 690°C. Apparently, water promotes the crystallization of the glass by lowering its viscosity [25].

Using IR spectroscpy, the effect of a precrystallization treatment on the water conctent in glass was evaluated for the samples revitrified in the gradient furnace for both the ambient air and the wet air conditions. The glass samples for the evaluation were at the vicinity of their liquidus temperature. For as-received samples, we found that the water content in glass was significantly reduced, by about 50%, as compared with the water concentration of untreated glasses, suggesting that water can easily escape from the glass during the devitrification. However, in the wet air, the water content of the samples, after the cycle of devitrification and vitrification, either remained about the same level or increased by about 45%.

4.5 Viscosity of Glass Melts

Within experimental error, no detectable effect of water in glass on the viscosity of the glass melt was observed. In the investigated temperature range, many of the Si-O-Si bonds are broken by very high thermal energy, so that additional rupture of the Si-O-Si bridge by water has little further effect. In addition, the magnitude of the effect of water in glass on viscosity of the glass melt has been previously reported to be strongly dependent on the glass composition [26] with the larger effect being observed at lower temperature.

In this study, the dependence of the viscosity on the temperature can be fitted using the Fulcher equation as [27]:

$$\log \eta = A + B/[T(^{o}C) - T_o] \quad (18)$$

where η is the viscosity (Pa.s) and A, B and T_o are the constants obtained by the regression analysis through the best fit of the experimental data. To obtain the best fit, the previously reported viscosity, $10^{11.3}$ Pa.s [28], at the glass transition temperature was used. Figures 29(A-C) represent the comparison between the experimental data and the fitting curves of Equation (17). Good agreement is apparent. Appendix C2 summarizes the fitting parameters (A,B,T_o) with one standard deviations.

4.6 Electrical Conductivity

From Figures 24(A-C), which illustrate the electrical conductivity versus the water concentration in glass at 1150 °C, an interesting trend is observed. At least for CVS2-18 and CVS2-52, the data in Figures 24(A-B) suggest that the conductivity initially decreases and then increase with increasing water content in the glass. For CVS2-74 shown in Figure 24(C), a similar trend might exist except for one datum point. The profile of electrical conductivity versus water content at high temperature obtained in this study appears to be similar to those previously reported at low temperature for silicate glasses [29,30]. The extent of variation for the σ-C_{OH} in this case is very small, which is also expected at high temperatures as shown by other reported data [31]. Figure 30 represents the logarithmic conductivity versus water content for silicate glasses [29,30]. It is apparent that there exists a particular water concentration level, above which the electrical conductivity increases. This is similar to the mixed alkali effect. Figure 31 represents the influence of temperature on the mixed alkali effect, indicating the higher the temperature, the smaller the effect [31].

For better comparison with the temperature dependence of viscosity of the glass melt, electrical resistivity of the glass melts was also fitted using the Fulcher equation as [27]:

$$\log \rho = A' + B'/[T(^{o}C) - T_o] \quad (19)$$

where ρ is the resistivity (ohm-m) and A',B' and T_o are the constants. For the limitted temperature range, the best fit was found by using the previously determined T_o values from viscosity for the corresponding samples (cf. Appendix C2). Figures 32(A-C) illustrates the comparison between the experimental data and the best fit curves according to Equation (19). Appendix D2 summarizes the fitting parameters (A', B' and T_o) for all glass melts. It is known that the constants, B, from the viscosity and, B', from resistivity are related to activation energies of the viscous flow and ionic motion, respectively. For the

simulated nuclear waste glasses investigated, data from Appendix C1.2 and Appendix D1.2 show that the ratio of B/B' is approximately 3.5.

5. Conclusions

Water content in simulated nuclear waste glasses, varied by changing the water vapor pressures during glass melting, had a measurable influence on the long term chemical (PCT), glass transition temperature, and electrical conductivity of glass melts. The effect on both the MCC-1 chemical durability of the glasses and viscosity of the glass melts were rather small. In addition, for the PCT and the glass transition temperature, some of the as-received glasses did not follows the general trends exhibited by other glasses with varied water content. This anomaly is probably due to inhomogeneity of the as-received glasses and a slight difference in glass composition between the as-received and other glasses. A significant amount of water was found to escape from the glass by pre-crystallization treatment in ambient air. The influence of a moisture atmosphere on the liquidus temperature was observed.

Reference

[1] Informations on the chemical compositions of the CVS2-18, 52 and 74 glasses were provided by Pacific Northwest Laboratory, Richland, WA , March, 1993.

[2] CRC Handbook of Chemistry and Physics, 56th edition, D-180, CRC Press, Cleveland, OH, (1975).

[3] H. Scholze, Glass Ind., **47**[11] 622 (1966).

[4] H. Franz, J. Amer. Ceram. Soc., **49**[9], 473 (1966).

[5] M.I. Nieto, A. Duran, J.M.F. Navarro and J.L.O. Mazo, J. Amer. Ceram. Soc. **67**[4], 242 (1984).

[6] J.L. Parsons and M.E. Milberg, J. Amer. Ceram: Soc., **43**[6], 326 (1960).

[7] G.A. Pasteur, J. Amer. Ceram. Soc., **56**[10] 548 (1973).

[8] A.D. Pearson, G.A. Pasteur and W.R. Northover, J. Mater. Sci.,**14**, 869 (1979).

[9] MCC-1 Static Leach Test Method, Materials Characterization Center Pacific Northwest Laboratory, Richland, WA 99352, December 20, 1985.

[10] Beckman Handbook of Spectral Line Characteristics for the DC Plasma/Echelle Systems, SPEX Industries, Inc., Metuchen, NJ.

[11] MCC-TP-19: Leaching Tests Using The PCT Test Method
Materials Characterization Center, Pacific Northwest Laboratory, Richland WA 99352, October 10, 1990.

[12] C.T. Moynihan, A.J. Easteal, J. Wilder and J. Tucker, J. Phys. Chem. **78[26]** 2673 (1974).

[13] C.T. Moynihan and S. Cantor, J. Chemical Phys., **48[1]** 115 (1968).

[14] E.N. Boulos, J.W. Smith and C.T. Moynihan, Gastenchnische Berichte Zeitschrift fur Glaskunde, XII Internationaler Glaskongreβ, **56K Bd.1** 509 (1983).

[15] P.B. Macedo, C.T. Moynihan and R. Bose, Phys. Chem. Glass., **13[6]** 171 (1972).

[16] H.C. Parker and E.W. Parker, J. Amer. Chem. Soc., **46**, 312 (1924).

[17] A.J. Moulson and J.P. Roberts, Trans. Farad. Soc., **57**, 1208 (1961).

[18] V. McGahay, Ph.D. thesis, Rensselaer Polytechnic Institute, Troy, NY, 1992.

[19] R.J. Charles, J. Appl. Phys., **11**, 1549 (1958).

[20] T. Advocal, J.L. Crovisier, E. Vermaz, G. Ehret and H. Charpentier Mater. Res. Soc. Symp. Proc. **Vol. 212**, 57 (1991).

[21] N.E. Bibler and J.K. Bates, Mater. Res. Soc. Symp. Proc. **Vol. 176** 327 (1990).

[22] D.E. Clark, A. Lodding, H. Odelius and L.O. Werme, Mater. Sci. Eng. **91**, 241 (1987).

[23] M. Tomozawa, M. Takata, J. Acocella, E.B. Watson and T. Takamori Yogyo-Kyokai-Shi, **91[8]** 377 (1983).

[24] P. Hrma, Pacific Northwest Laboratory, Richland, WA 99352 (private communication May, 1994).

[25] E.N. Boulos, R.P. DePaula, O.H. El-Bayoumi, N. Lagakos, P.B. Macedo C.T. Moynihan and S.M. Rekhson, J. Amer. Ceram. Soc., **63[9-10]** 496 (1980).

[26] J.M. Jewell, C.M. Shaw and J.E. Shelby, J. Non-Cryst. Solid.,**152** 32 (1993).

[27] G.S. Fulcher, J. Amer. Ceram. Soc., **8**, 339 (1925).

[28] C.T. Moynihan, J. Amer. Ceram. Soc., **76[5]** 1081 (1993).

[29] M. Takata, J. Acocella, M. Tomozawa and E.B. Watson, J. Amer. Ceram. Soc. **64[12]** 719 (1981).

[30] M. Takata, M. Tomozawa and E.B. Watson, J. Amer. Ceram. Soc. **65**[2] 91 (1981).

[31] C.T. Moynihan, N.S. Saad, D.C. Tran and A.V. Lesikar, Amer. Ceram. Soc. **63**, 458 (1980).

Table I Chemical Compositions of the Simulated Nuclear Waste Glasses [1]

Glass	CVS2-18	CVS2-52	CVS2-74	
Oxide	Content (wt%)			Chemicals
SiO_2	53.53	60.00	56.60	SiO_2
B_2O_3	10.53	8.17	7.81	H_3BO_3
Na_2O	11.25	4.50	6.64	Na_2CO_3
Li_2O	3.75	7.88	7.13	Li_2CO_3
CaO	0.83	0.08	0.79	$CaCO_3$
Fe_2O_3	7.19	7.20	3.34	Fe_2O_3
Al_2O_3	2.31	2.33	8.16	Al_2O_3
MgO	0.34	0.09	0.32	MgO
ZrO_2	3.85	3.85	0.05	ZrO_2
Others	5.92	5.90	9.16	CVS Mix

Table II MCC-1 Test Matrix for the Simulated Nuclear Waste Glasses

Number of specimens	CVS2-18	CVS2-52	CVS2-74
as-received	3	3	3
93 mmHg @	3	3	3
355 mmHg @	3	3	3
760 mmHg @	3	3	3

@ The value represents the saturated water vapor pressure under which these glasses were remelted.

Table III Selective Chemical Compositions and the Related Mass Fraction of Metal Elements for the Simulated Nuclear Waste Glasses

Glass	CVS2-18	CVS2-52	CVS2-74
SiO_2 (wt%)	53.53	60.00	56.60
B_2O_3 (wt%)	10.53	8.17	7.81
Li_2O (wt%)	3.75	7.88	7.13
Na_2O (wt%)	11.25	4.50	6.64
f_{Si} (g)	0.2502	0.2805	0.2646
f_B (g)	0.0327	0.0254	0.0243
f_{Li} (g)	0.0174	0.0366	0.0331
f_{Na} (g)	0.0835	0.0334	0.0493

Table IV PCT Test Matrix for the Simulated Nuclear Waste Glasses

Number of specimens	CVS2-18	CVS2-52	CVS2-74
as-received	1	1	1
93 mmHg @	1	1	1
355 mmHg @	1	1	1
760 mmHg @	1	1	1

@ The value represents the saturated water vapor pressure under which these glasses were remelted.

Table V Hydroxyl IR Absorption Coefficient, (A/d), for the Simulated Nuclear Waste Glasses (as-received and remelted)

Units: abs/cm

Glass Water vapor	CVS2-18	CVS2-52	CVS2-74
as-received	5.30	5.30	5.75
93 mmHg @	2.45	2.34	2.12
355 mmHg @	4.47	4.12	3.88
760 mmHg @	9.02	8.94	5.75

@ The value represents the saturated water vapor pressure under which these glasses were remelted.

Table VI Determination of Extinction Coefficient of Hydroxyl Absorption by Dehydration Method for the Simulated Nuclear Waste Glasses

Glass	CVS2-18	CVS2-52	CVS2-74
W (mg)	80.12	55.10	77.74
d (μm)	418.0	294.0	418.0
ρ (g/cm^3)	2.69	2.63	2.61
$\Delta A/\Delta W$ (abs/g)	1226.6	1713.1	1874.8
ϵ_{OH} (lit/mol-cm)	7.84	10.99	12.05
ϵ'_{OH} (abs/cm-ppm)	1.24×10^{-3}	1.70×10^{-3}	1.85×10^{-3}

Table VII Hydroxyl Concentrations in the Simulated Nuclear Waste Glasses (as-received and remelted)

Units: ppm by wt

Glass Water vapor	CVS2-18	CVS2-52	CVS2-74
as-received	4274	3118	3108
93 mmHg @	1976	1376	1146
355 mmHg @	3605	2424	2097
760 mmHg @	7274	5259	4438

@ The value represents the saturated water vapor pressure under which these glasses were remelted.

Table VIII Linear Regression Analysis of the Effect of Hydroxyl Concentration on the Dissolution of the Simulated Nuclear Waste Glasses using the PCT Method

10^5 $(NL)_i$ / C_{OH} $(g/m^2/ppm)$ # Element				
Glass	Li	B	Na	Si
CVS2-18	4.3±0.9 (0.96)&	2.8±0.7 (0.95)	4.5±0.9 (0.97)	0.6±0.2 (0.90)
CVS2-52	1.7±1.0 (0.73)	2.0±0.4 (0.97)	0.7±0.4 (0.72)	0.2±0.04 (0.96)
CVS2-74	4.1±0.1 (0.99)	1.9±0.4 (0.96)	1.3±0.4 (0.93)	1.0±0.1 (0.98)

The regression analyses did not include the data for as-received glasses.
& The value in parenthsis is the linear regression coefficient, r^2.

Table IX DSC Glass Transition Temperatures of the Simulated Nuclear Waste Glasses with Various Water Contents (Heating rate: 10 °C/min)

Glass	CVS2-18	CVS2-52	CVS2-74
93 mmHg@	488	476	474
355 mmHg@	484	476	467
760 mmHg@	471	473	465
as-received@	486	476	461

@ The values represent the water vapor pressure at which the glasses were remelted.

Table X Liquidus Temperature of the Simulated Nuclear Waste Glasses *

Glass	Ambient air@ (°C)	355 mmHg water vapor# (°C)
CVS2-18	842	871
CVS2-52	923	946
CVS2-74	852	872

* All samples were pre-heat-treated at 690 °C for 24 hr in either ambient air or 355 mmHg water vapor.
@ As-received glass samples were used.
# Glass samples used were previously remelted at 1150 °C under 355 mmHg water vapor.

Figure 1 A schematic diagram of experimental set-up for melting glass under controlled water vapor pressure

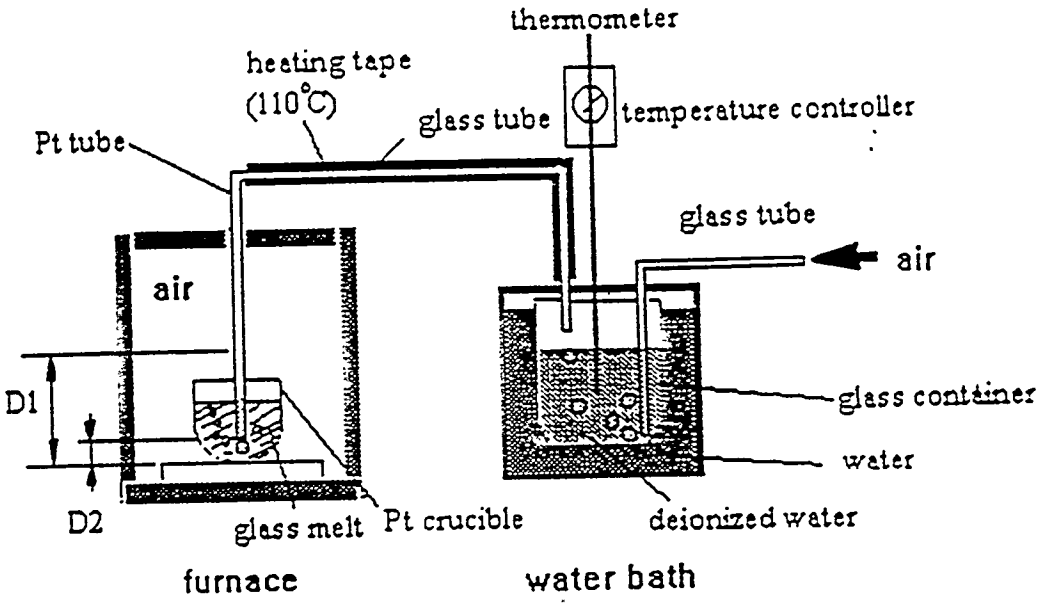

Figure 2 IR spectra of three as-received glasses (IR absorbance is normalized by the specimen thickness).

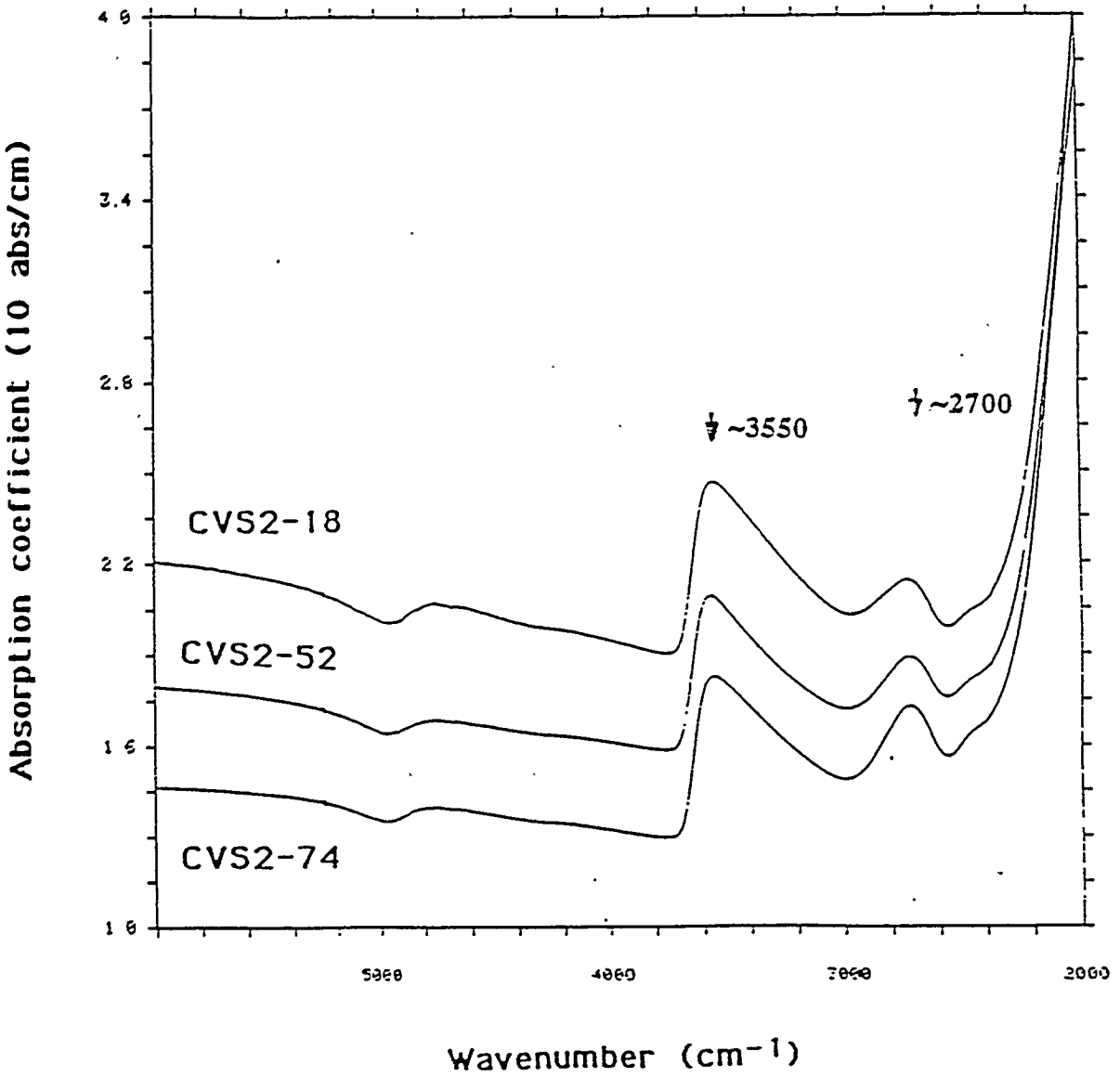

Figure 3 Caliberation curves for Beckman Spectraspan V Emission Spectrometer using SPEX standard solutions of Si, B, Li and Na for MCC-1.

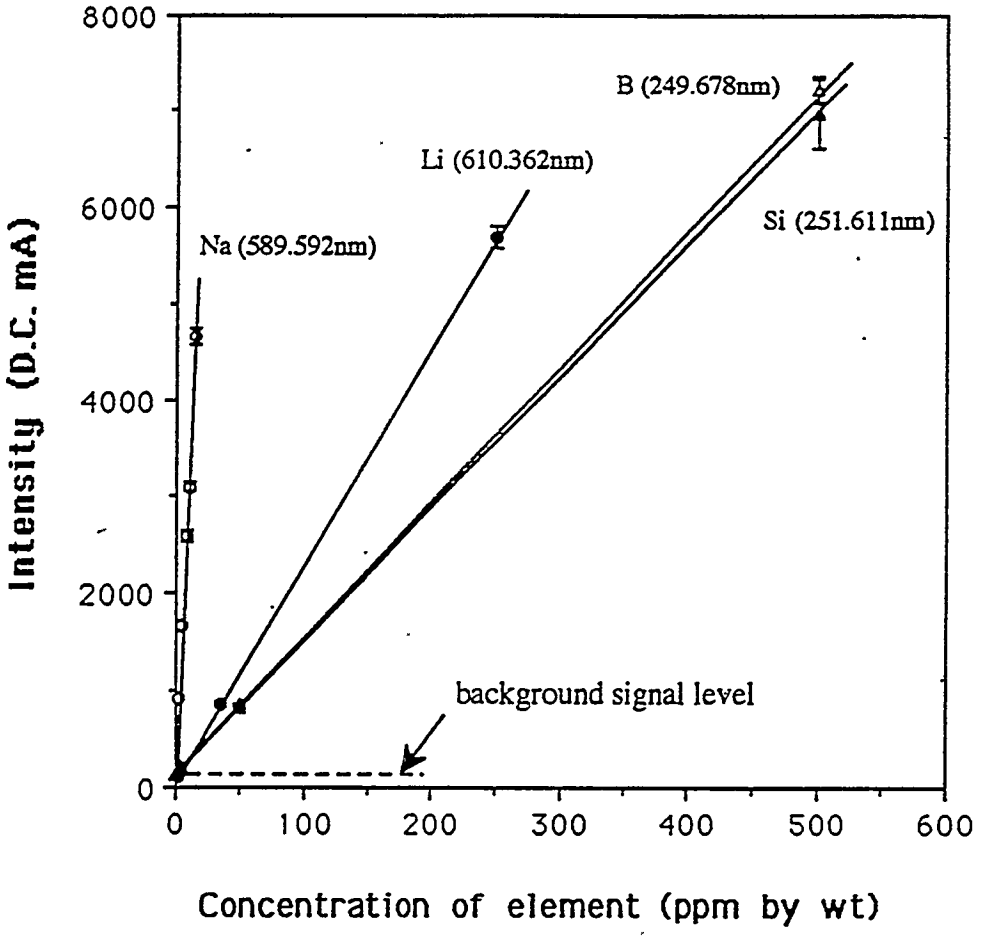

Figure 4 Calibration curves for Beckman Spectraspan V Emission Spectrometer using SPEX standard solutions of Si, B, Li and Na for PCT.

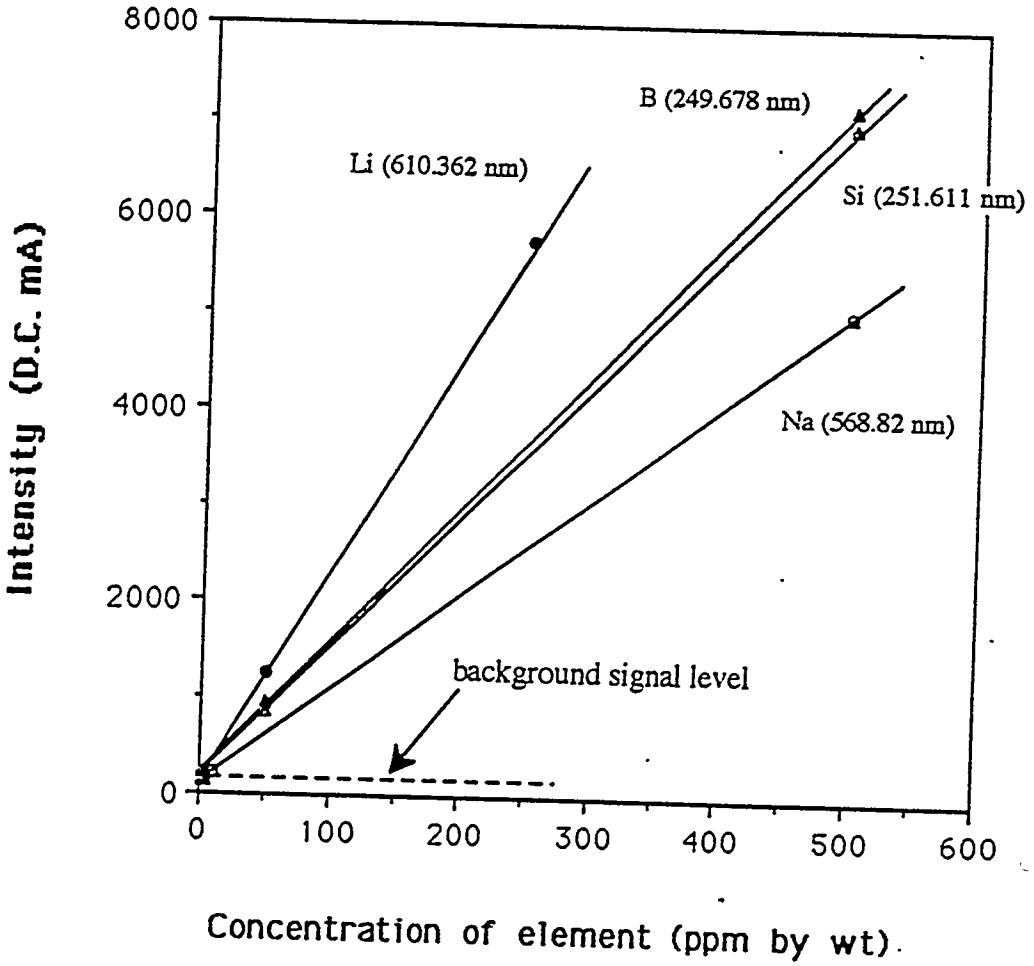

Figure 5 DSC spectrum of NBS standard SRM711 glass (obtained under heating rate of 10°C/min).

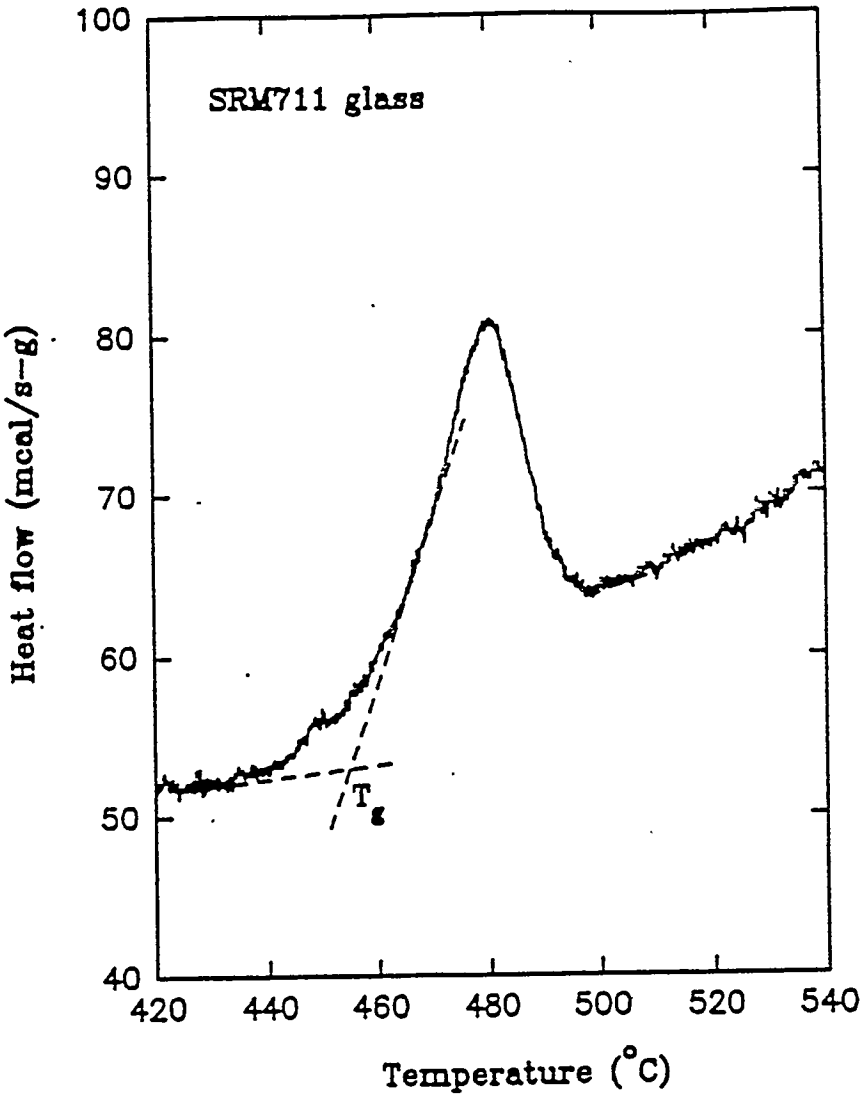

Figure 6 Temperature calibration curves for Lindberg 3–zone tube furnace.

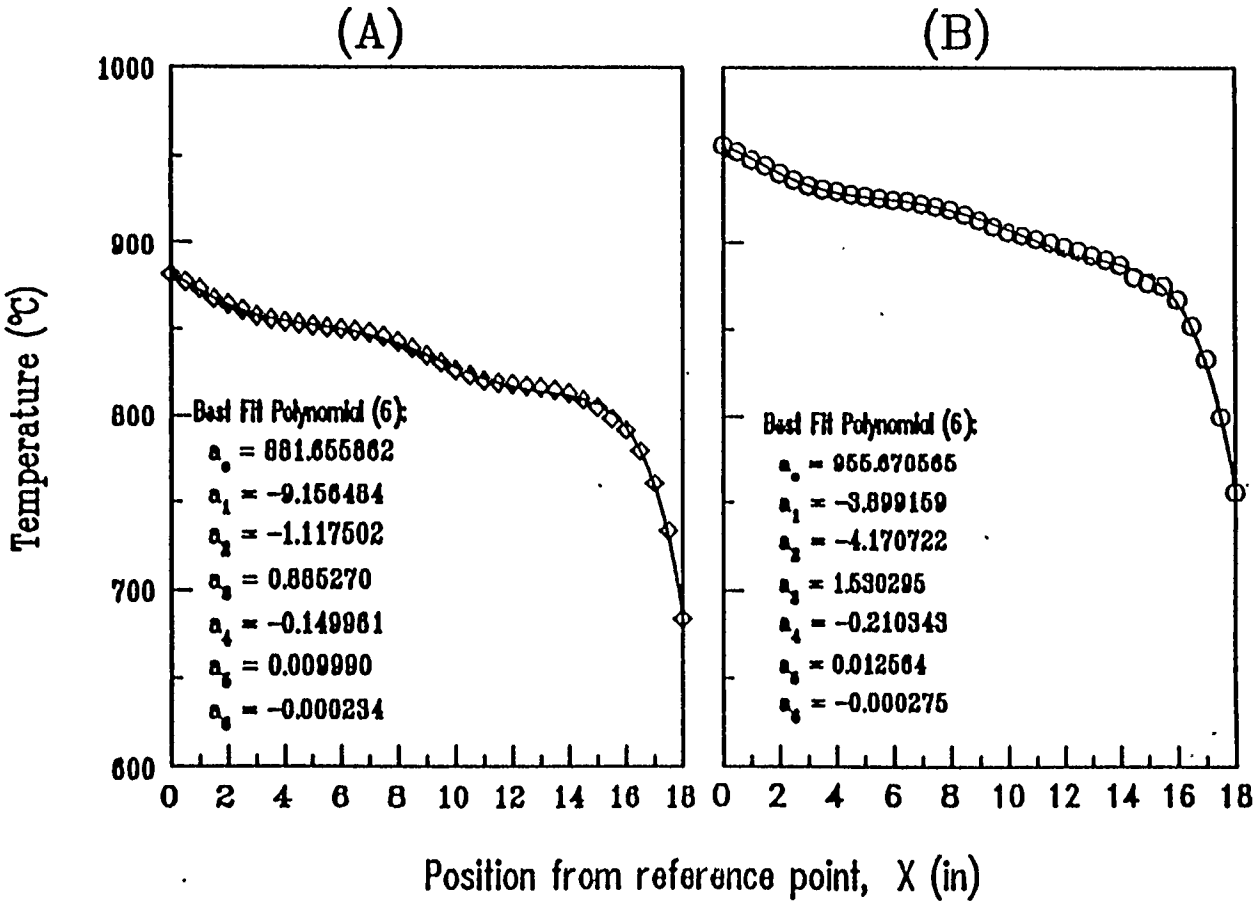

Figure 7 Geometry of spindle for viscosity measurement.

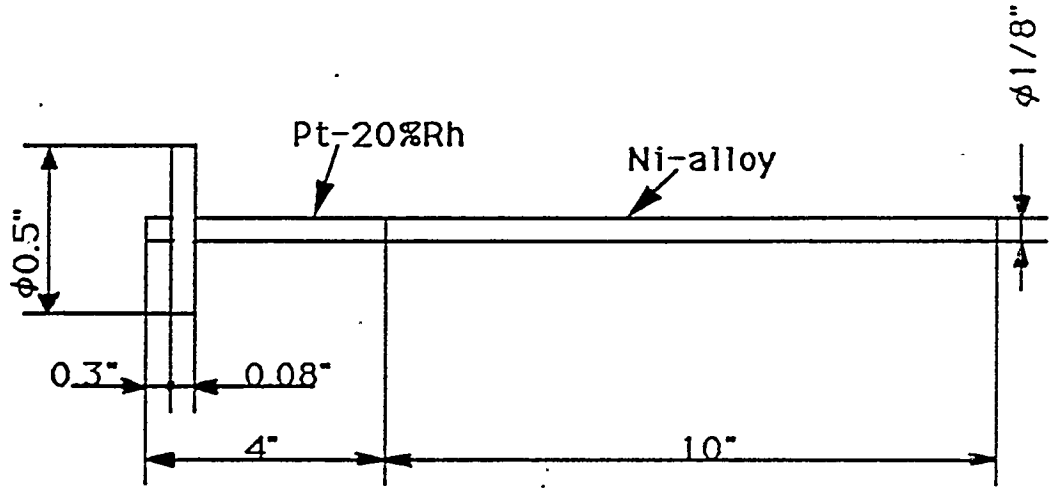

Figure 8 Determination of the cell constant using standard oils. (immersion depth : 0.9")

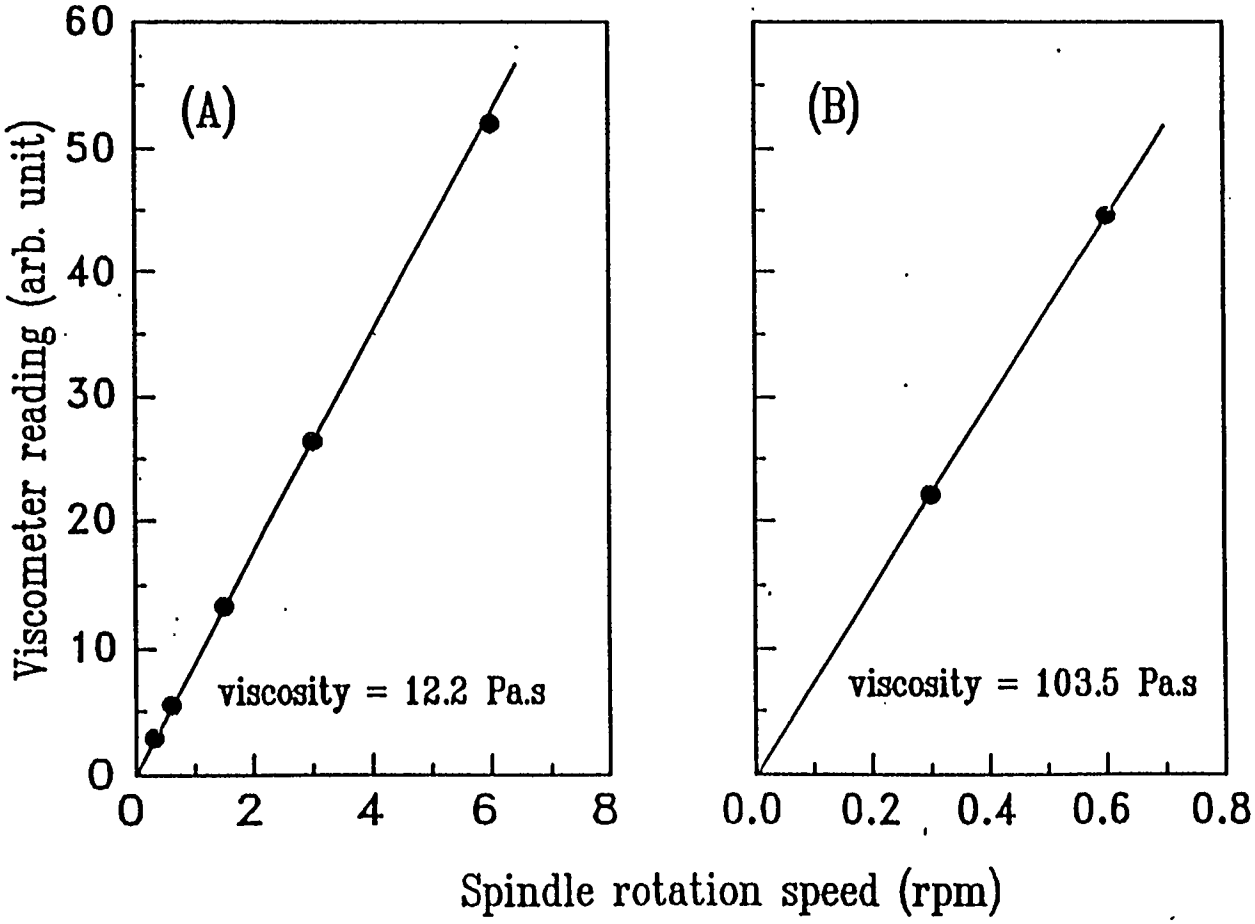

Figure 9 Z'–Z'' plot of standard KCl solutions (immersion depth : 0.7")

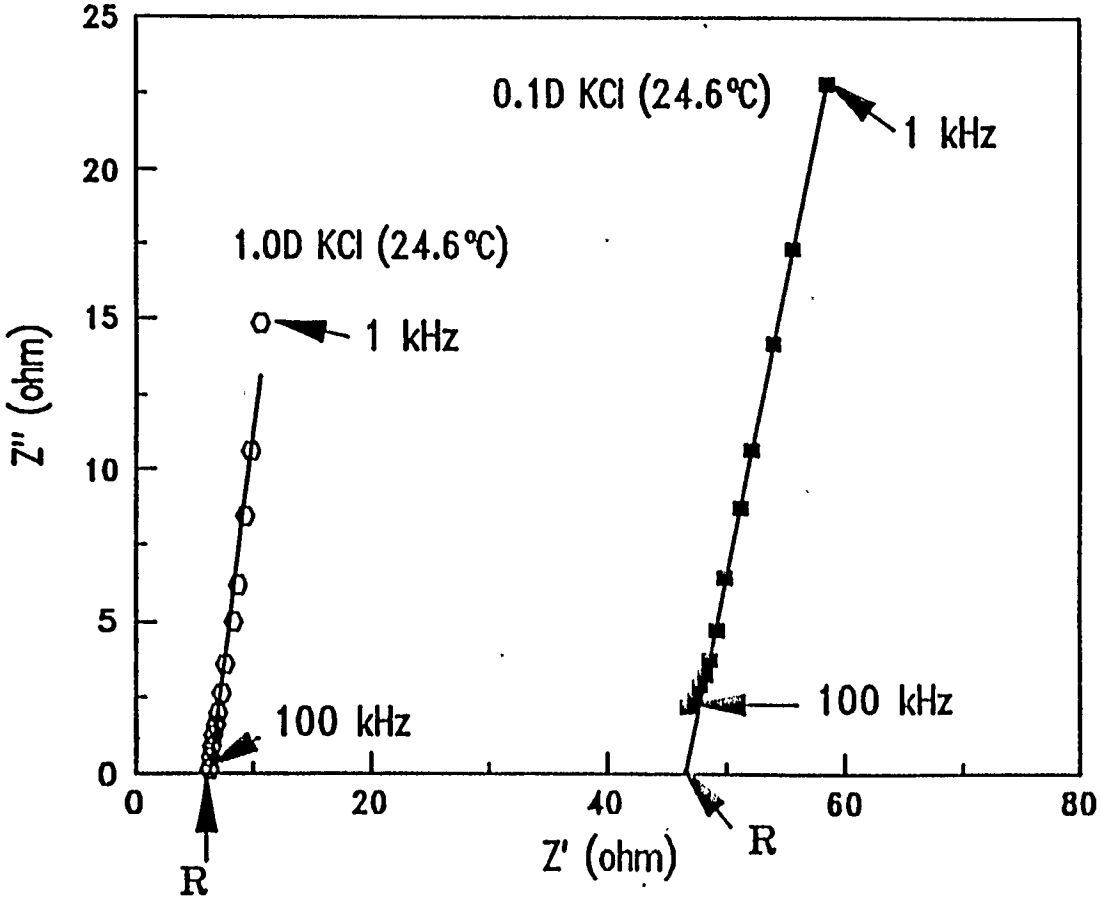

Figure 10 Hydroxyl IR absorbance as a function of specimen thickness for the glasses with various water concentrations

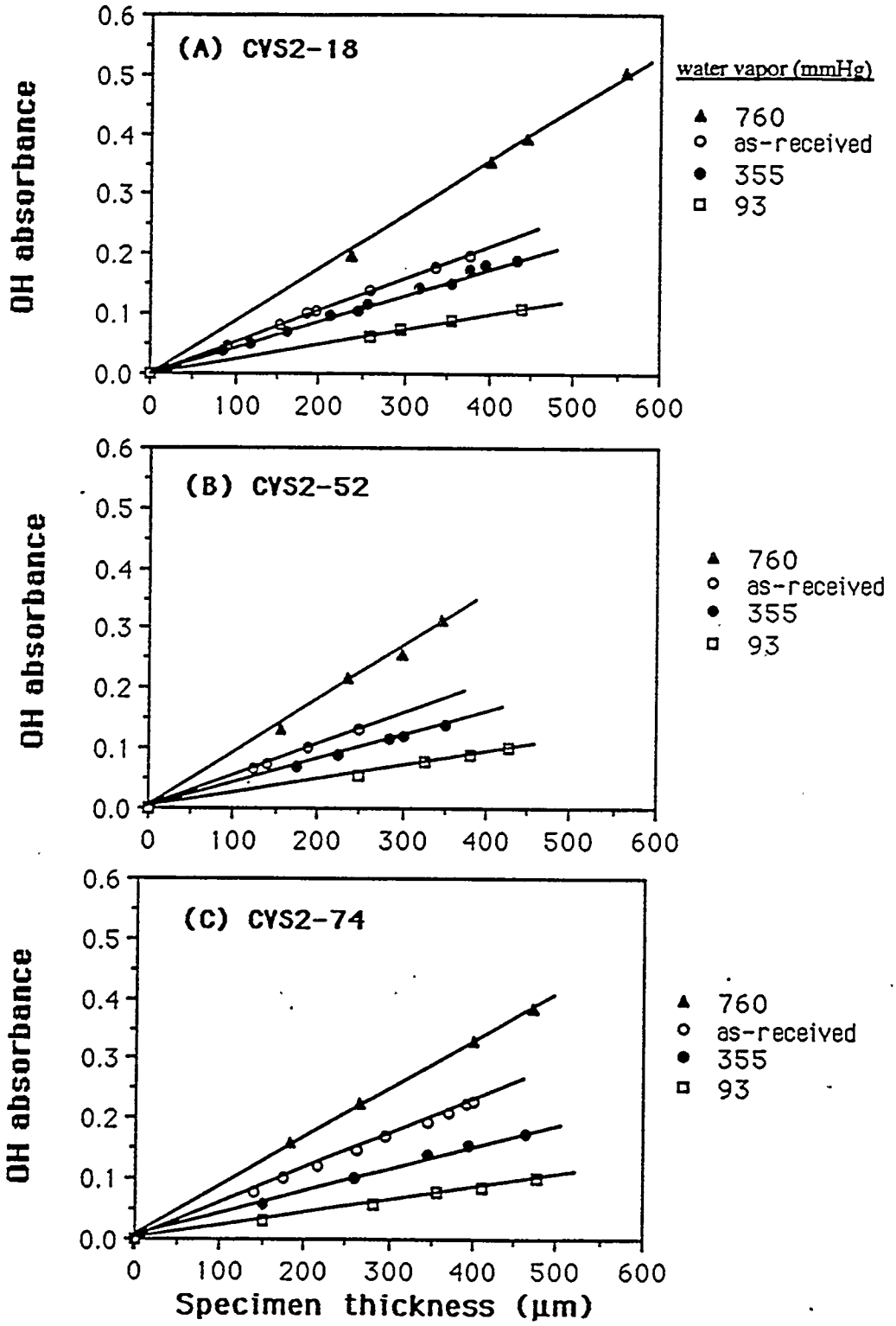

Figure 11 The change of OH absorbance as a function of the specimen weight loss for the simulated nuclear waste glasses.

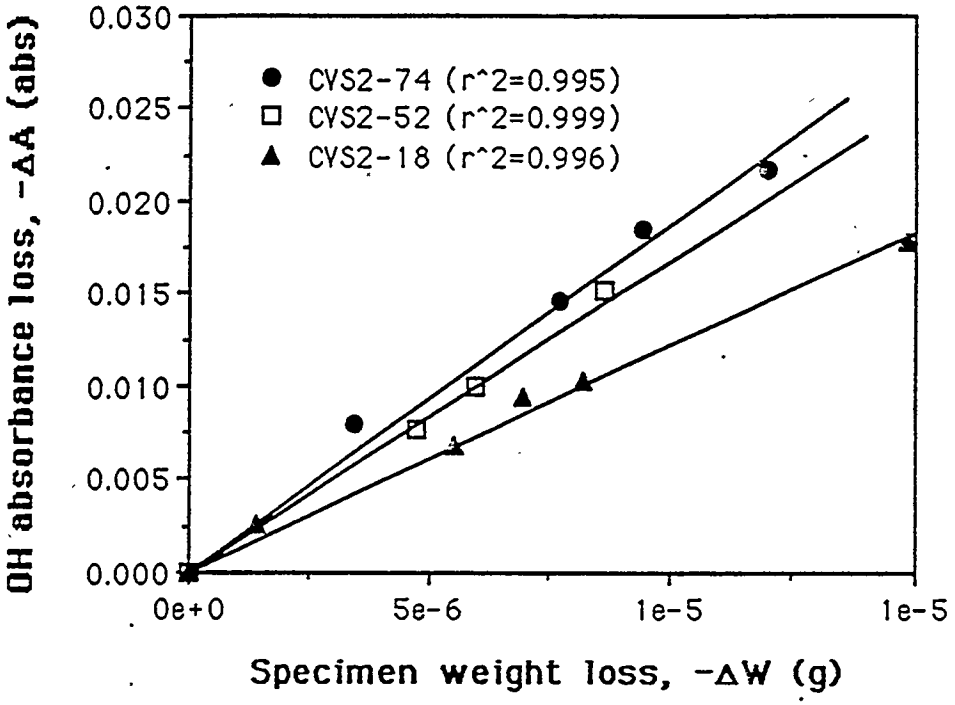

Figure 12 Hydroxyl concentration as a function of water vapor pressure under which the glasses were remelted.

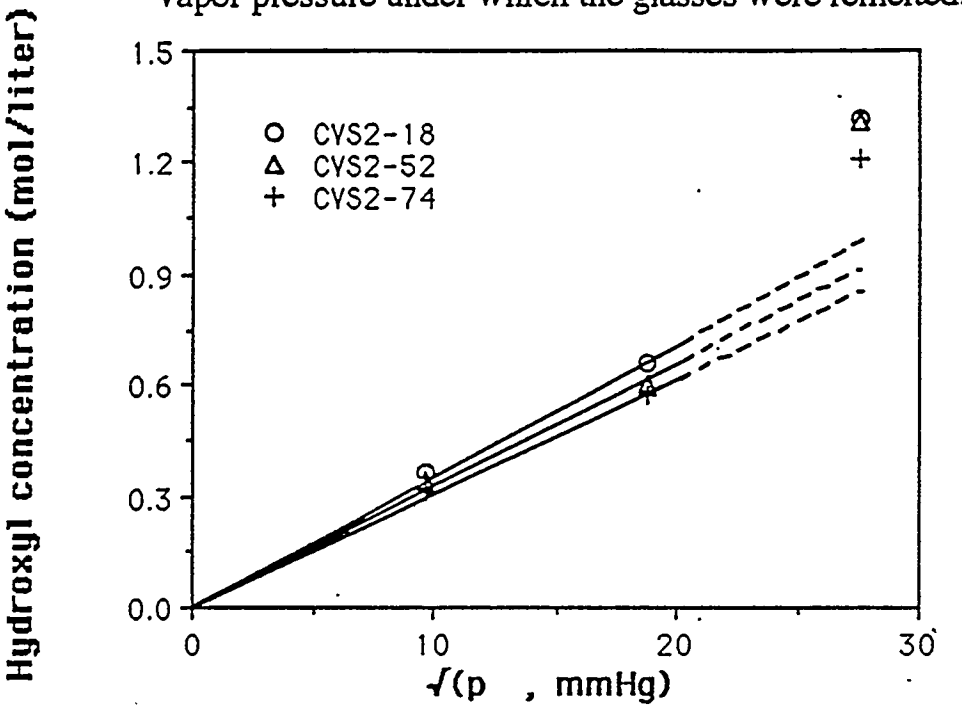

Figure 13 MCC-1 test for the simulated nuclear waste glasses having different water contents (DIW – 90 °C – 28 days – (SA/V) = 10 m^{-1}).

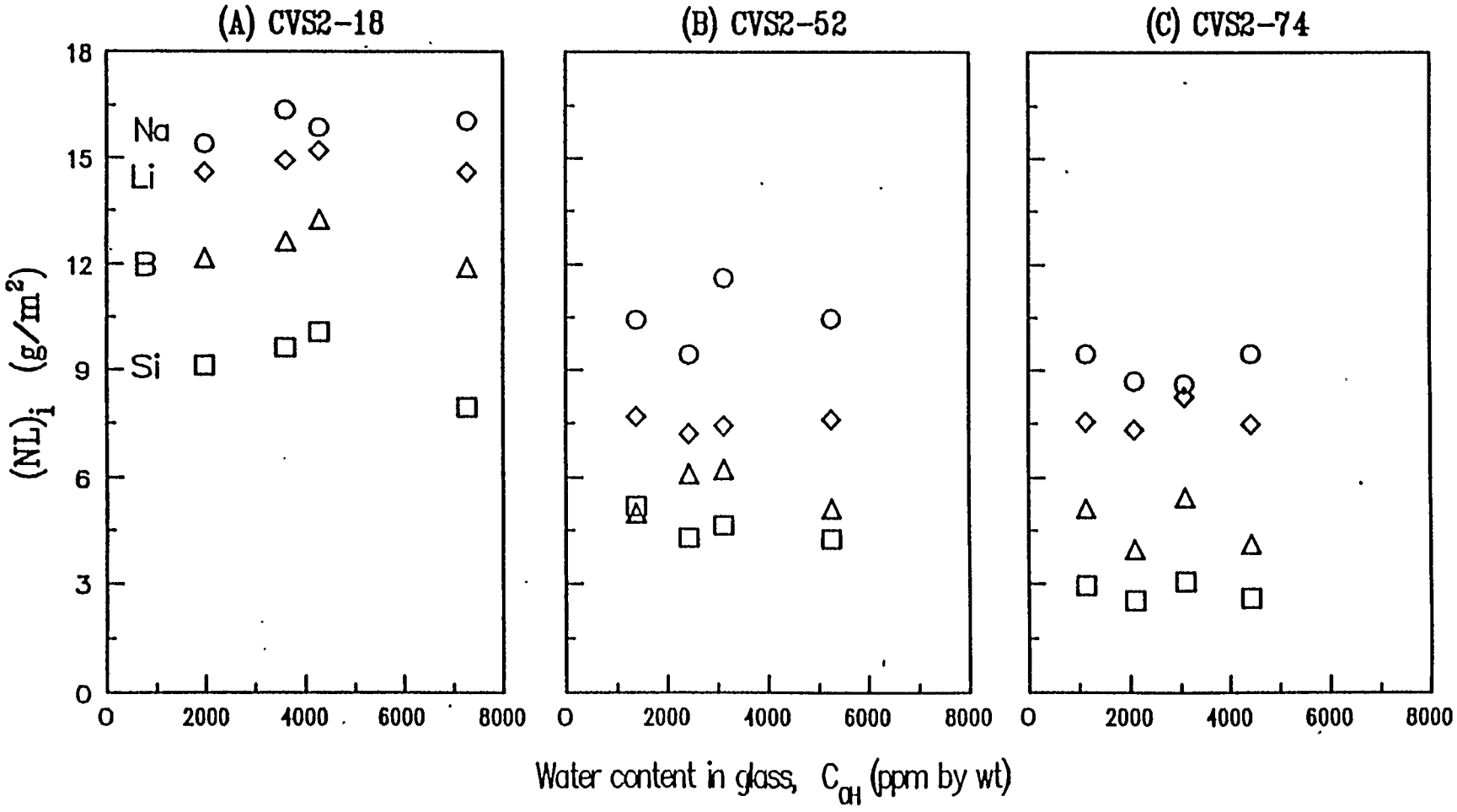

Figure 14 PCT test for the simulated nuclear waste glasses having different water contents (DIW – 90 ℃ – 7 days – (SA/V) = 2000 m^{-1}).

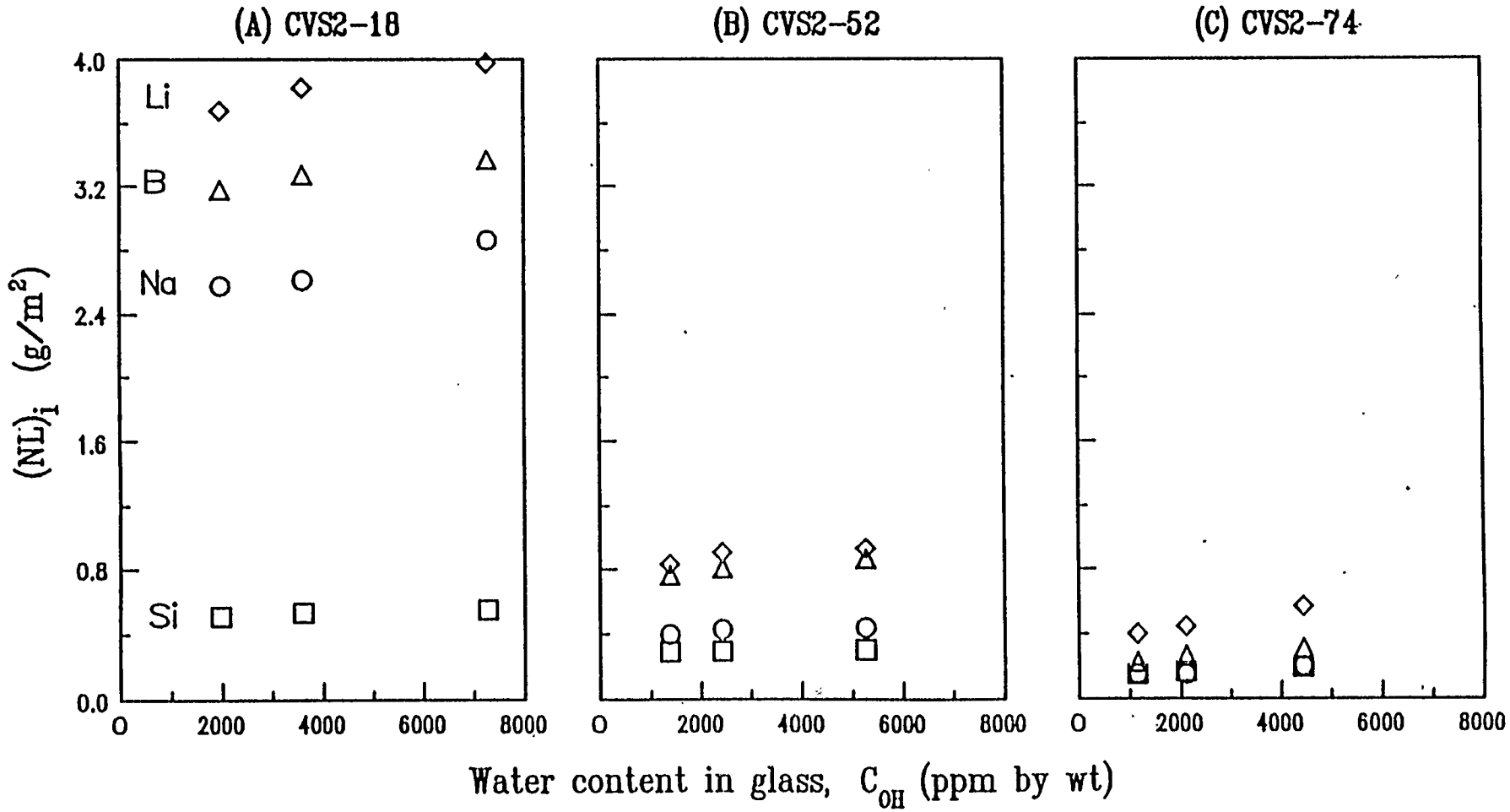

Figure 15 Normalized elemental mass loss of boron versus water concentration in the simulated nuclear waste glasses having different water contents.

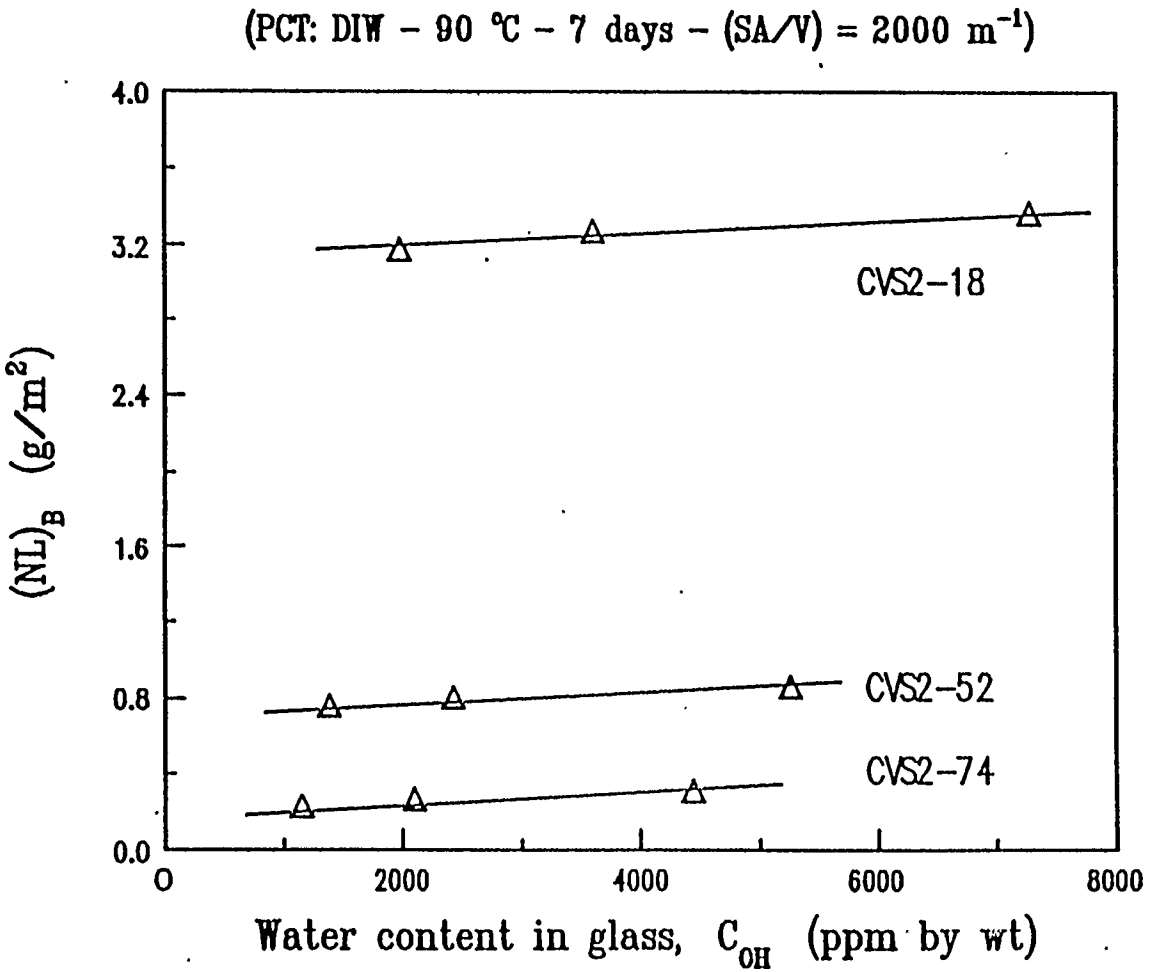

Figure 16 DSC scans of CVS2-18 glasses with different water concentrations (obtained under heating rate of 10°C/min)

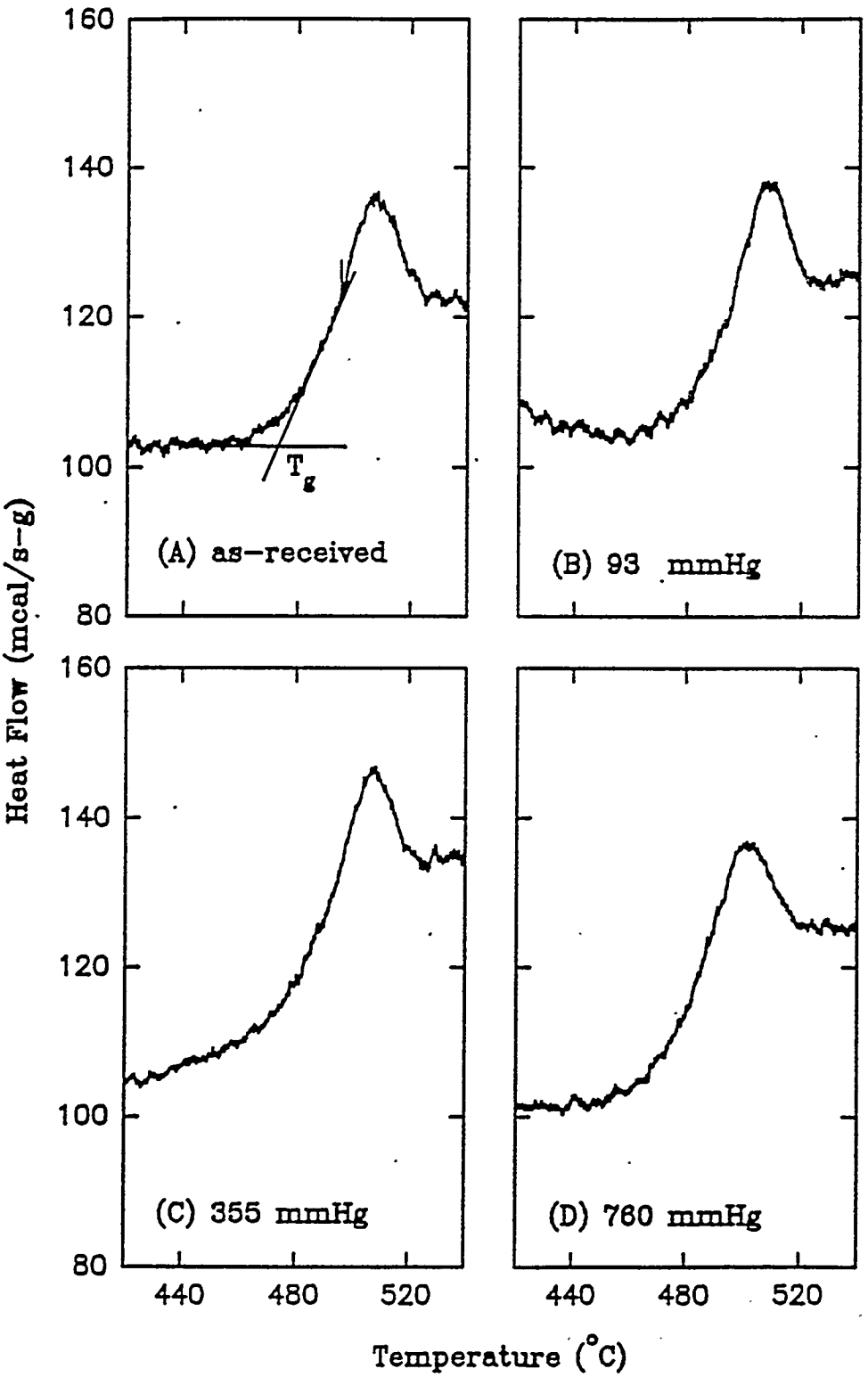

Figure 17 DSC scans of CVS2-52 glasses with different water concentrations (obtained under heating rate of 10°C/min).

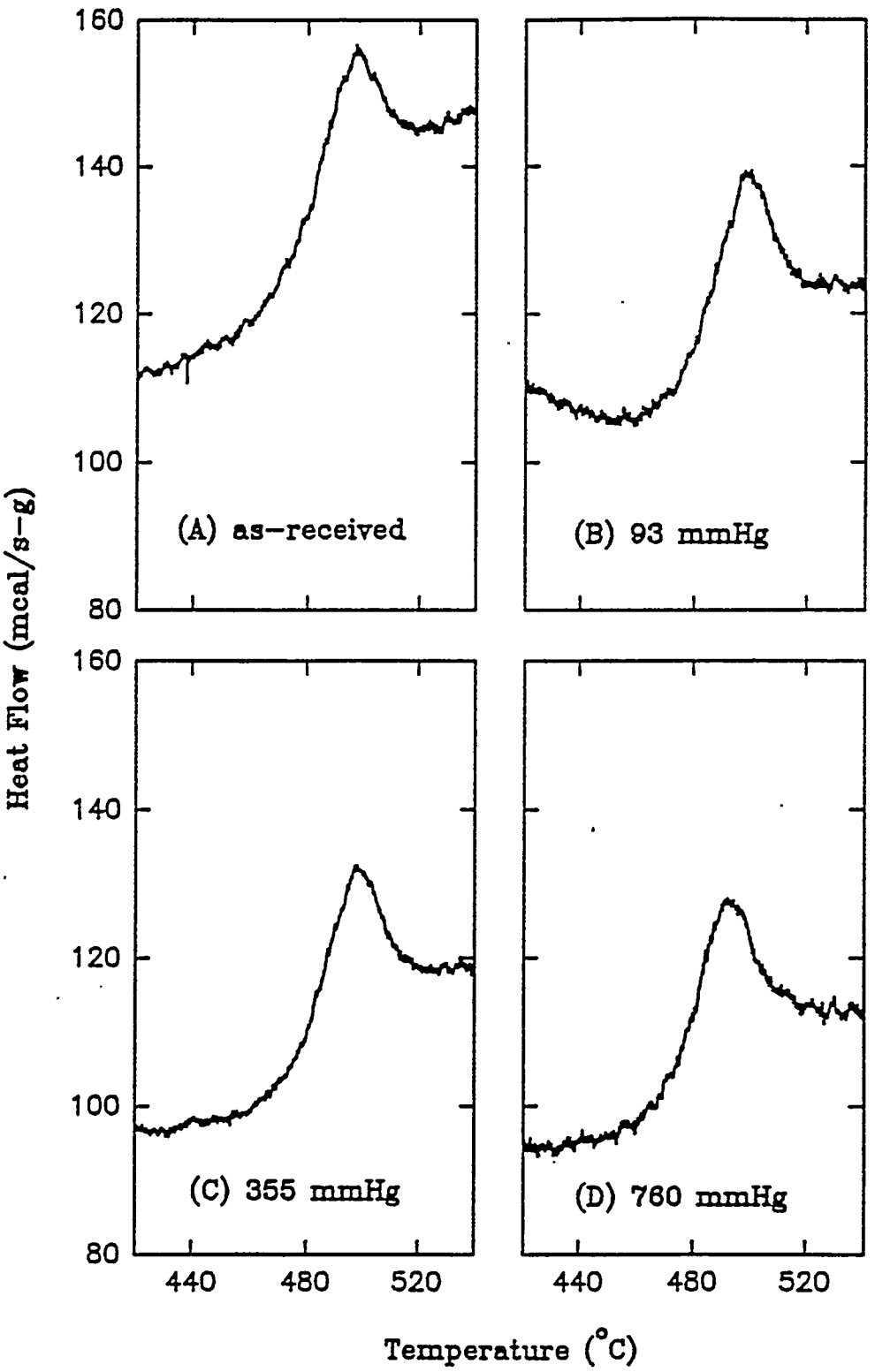

For Approval Of

Name	Approved	Date
DE Larson		6/1/94
JM Creer		6/1/94

Battelle
Pacific Northwest Laboratories
Battelle Boulevard
P.O. Box 999
Richland, Washington 99352
Telephone (509) 376-1982

May 27, 1994

Mr. R. W. Powell, Manager
High-Level Waste Program
Westinghouse Hanford Company
PO Box 1970
Richland, WA 99352

PNL-94-82

Dear Mr. Powell:

TRANSMITTAL OF MILESTONE PVTD-C94-03.01F, ISSUE UNIVERSITY WATER EFFECTS STUDY REPORT

The enclosed report from Rensselaer Polytechnic Institute, "Effects of Water on Properties of Simulated Nuclear Waste Glasses" is being submitted to meet the subject contractor milestone.

Technical questions should be directed to Pavel Hrma, 376-5092.

Very truly yours,

Eugene V. Morrey

E. V. Morrey, Task Manager
Process/Product Development
PNL Vitrification Technology Development Project

Attachment

Distribution:

RL - ST Burnum w/o att
M Dev w/ att
GH Sanders w/o att

TDPO - GH Beeman w/o att
JA Carr w/ att

WHC - TWRS DPC
RP Colburn
RL Gibby
ET Weber

PNL - JM Creer
ML Elliott
C Franks
GA Jensen
BM Johnson w/o
DA Lamar
DE Larson
BD Slonecker
GL Smith
PA Smith
KD Wiemers
File/LB

For Approval Of

Name	Approved	Date
DE Larson		6/1/94
JM Creer		6/1/94

Battelle
Pacific Northwest Laboratories
Battelle Boulevard
P.O. Box 999
Richland, Washington 99352
Telephone (509) 376-1982

May 27, 1994

Mr. R. W. Powell, Manager
High-Level Waste Program
Westinghouse Hanford Company
PO Box 1970
Richland, WA 99352

PNL-94-82

Dear Mr. Powell:

TRANSMITTAL OF MILESTONE PVTD-C94-03.01F, ISSUE UNIVERSITY WATER EFFECTS STUDY REPORT

The enclosed report from Rensselaer Polytechnic Institute, "Effects of Water on Properties of Simulated Nuclear Waste Glasses" is being submitted to meet the subject contractor milestone.

Technical questions should be directed to Pavel Hrma, 376-5092.

Very truly yours,

Eugene V. Morrey

E. V. Morrey, Task Manager
Process/Product Development
PNL Vitrification Technology Development Project

Attachment

Distribution:

RL - ST Burnum w/o att
M Dev w/ att
GH Sanders w/o att

TDPO - GH Beeman w/o att
JA Carr w/ att

WHC - TWRS DPC
RP Colburn
RL Gibby
ET Weber

PNL - JM Creer
ML Elliott
C Franks
GA Jensen
BM Johnson w/o
DA Lamar
DE Larson
BD Slonecker
GL Smith
PA Smith
KD Wiemers
File/LB

Figure 18 DSC scans of CVS2-74 glasses with different water concentrations (obtained under heating rate of 10°C/min).

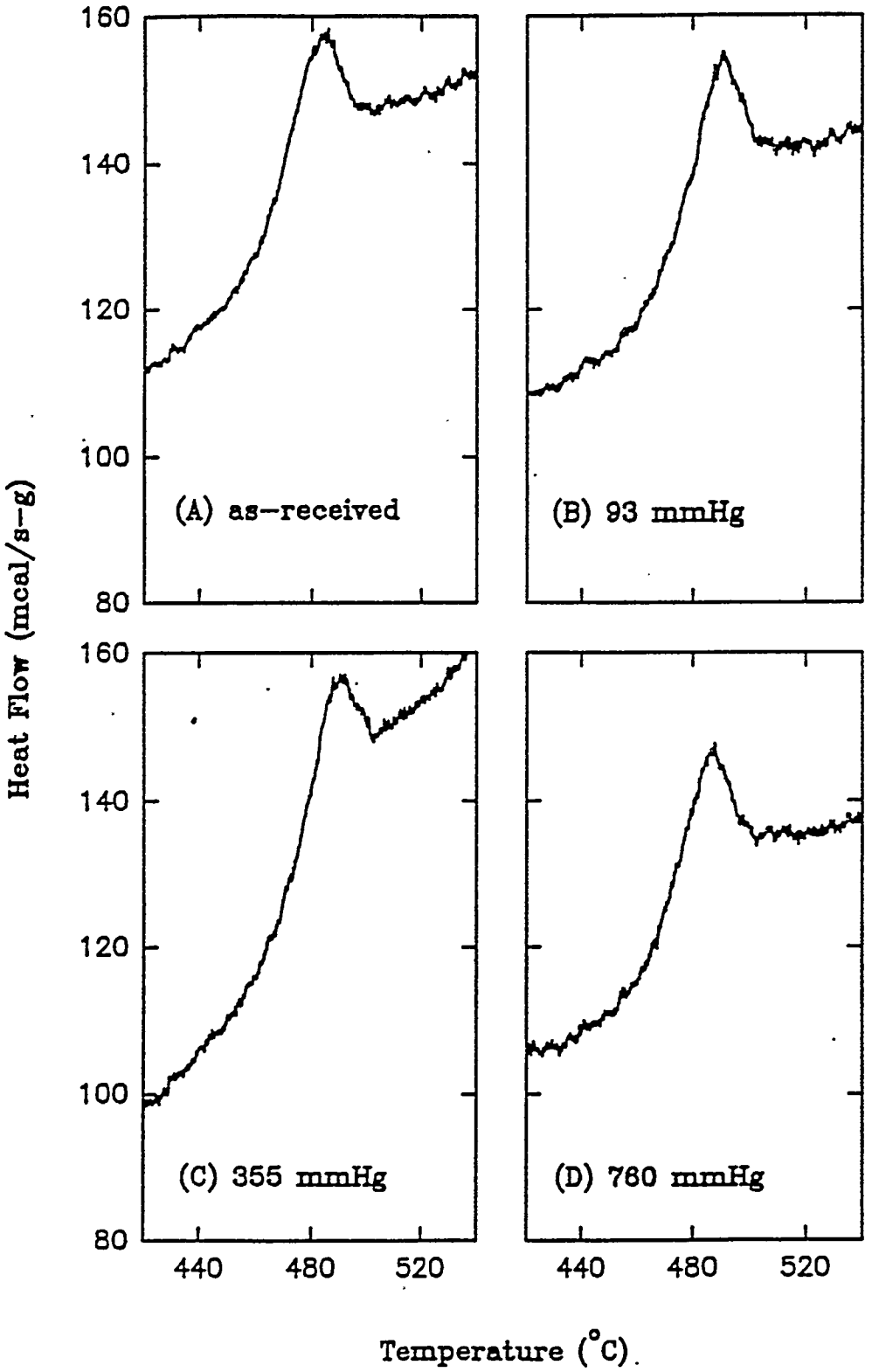

Figure 19 X-ray diffraction patterns of as-received glasses heat-treated at 690℃ in ambient air for 24 hr.

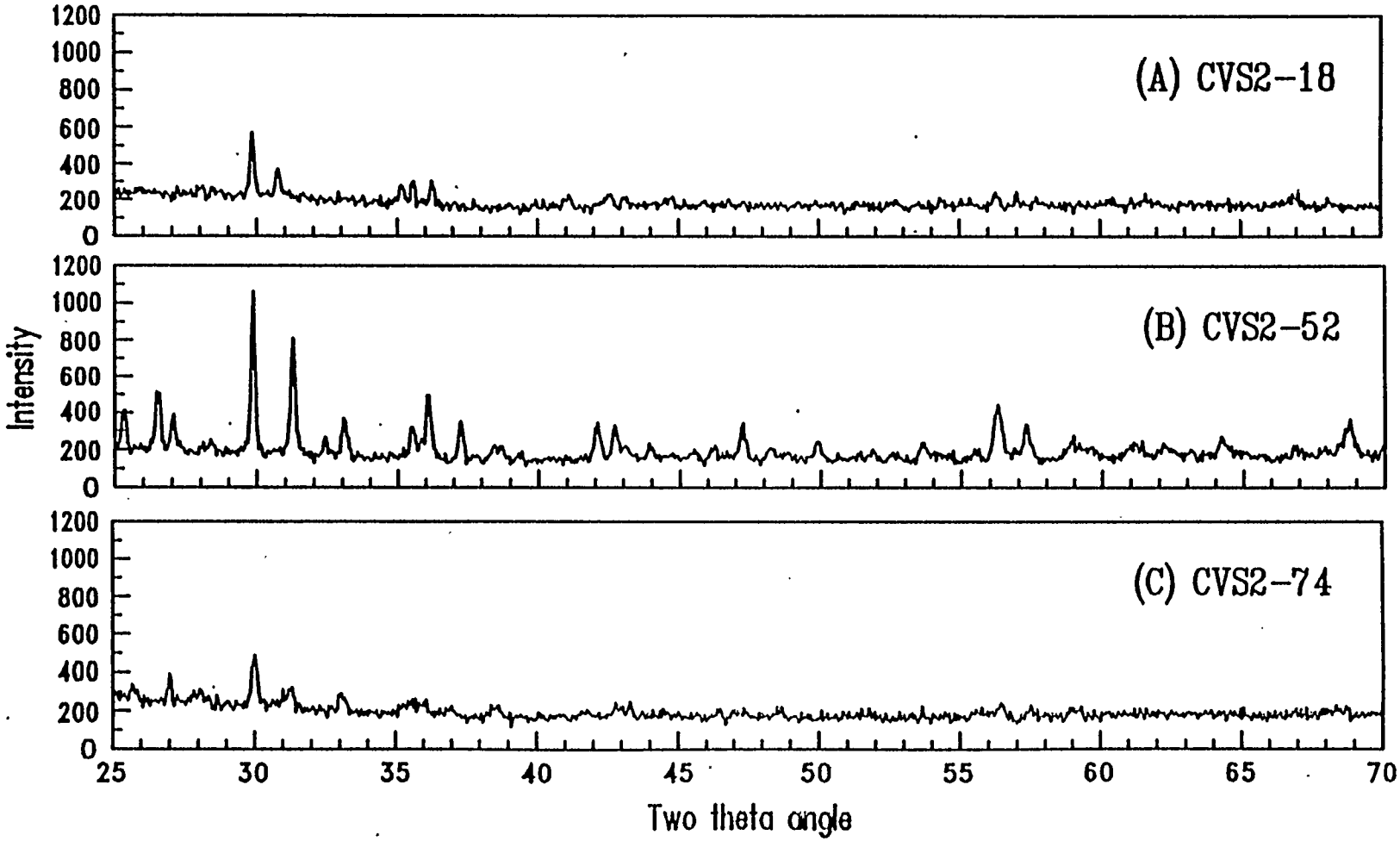

Figure 20 X-ray diffraction patterns of glasses remelted under 355 mmHg water vapor and then heat-treated at 690 ℃ in 355 mmHg water vapor for 24 hr.

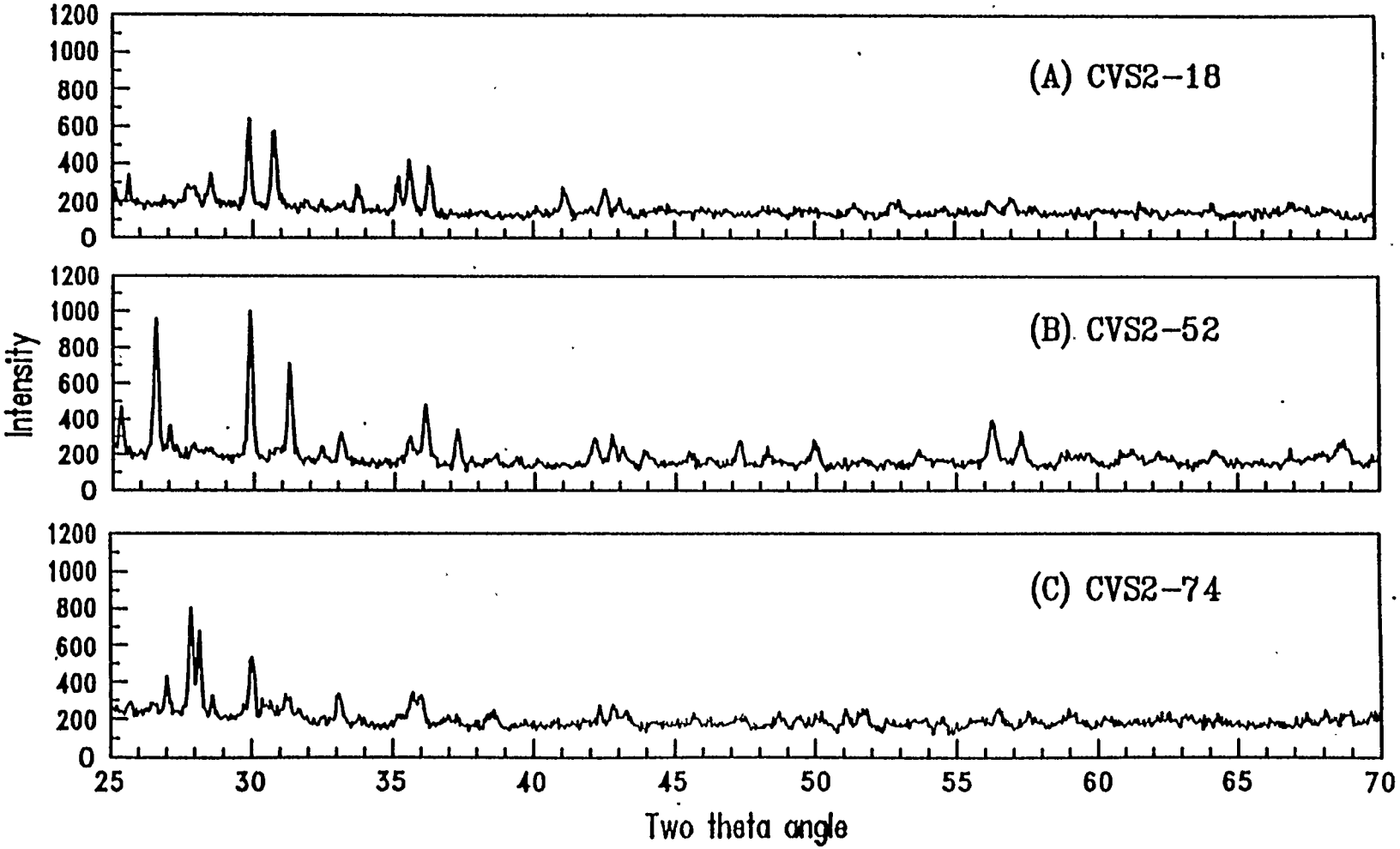

Figure 21 Viscosity of the glass melts as a function of temperature for the simulated nuclear waste glasses having different water contents.

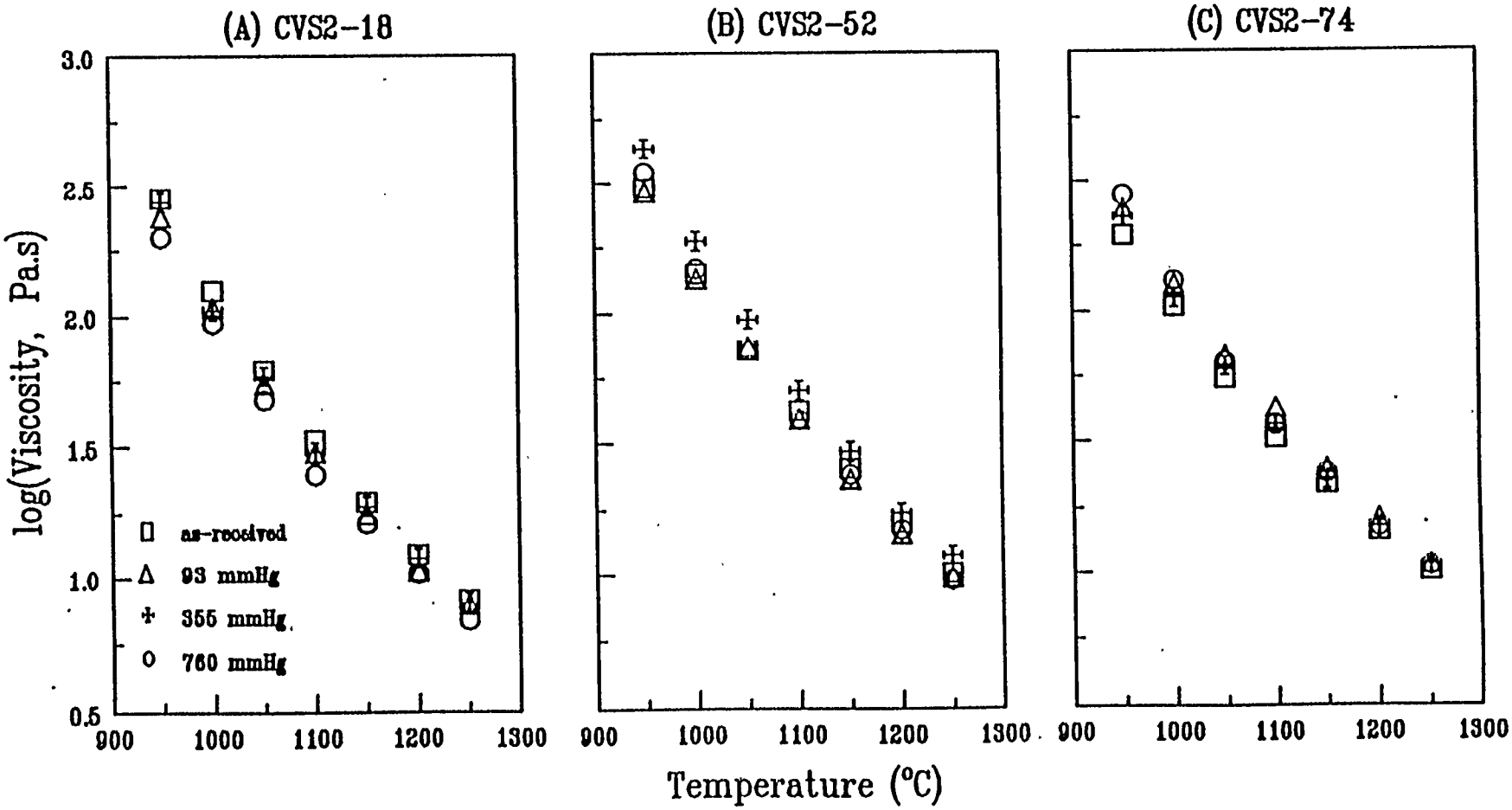

Figure 22 Viscosity versus water concentration in glass at 1150°C

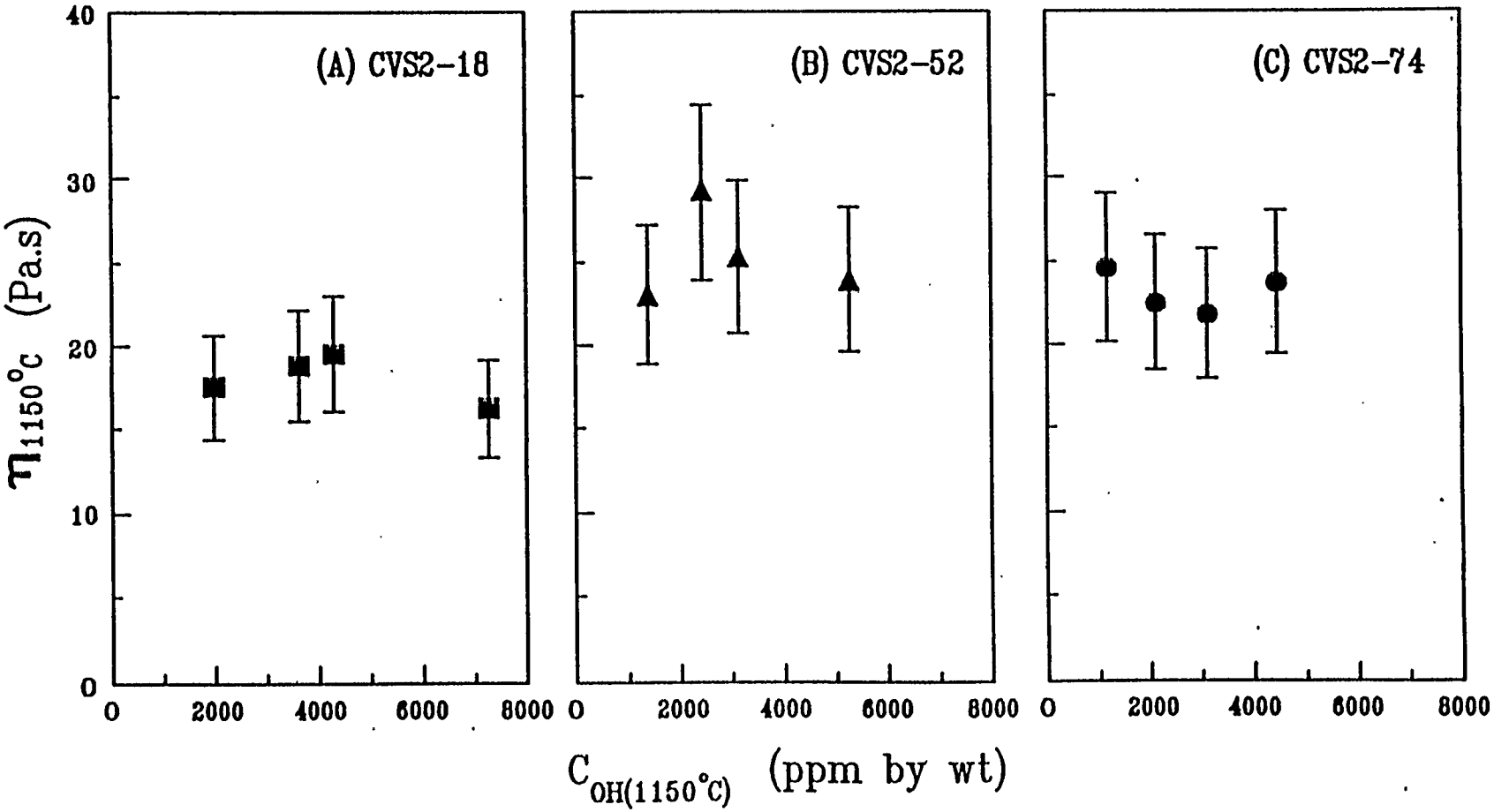

Figure 23 Electrical resistivity as a function of temperature
for the simulated nuclear waste glasses having different water contents.

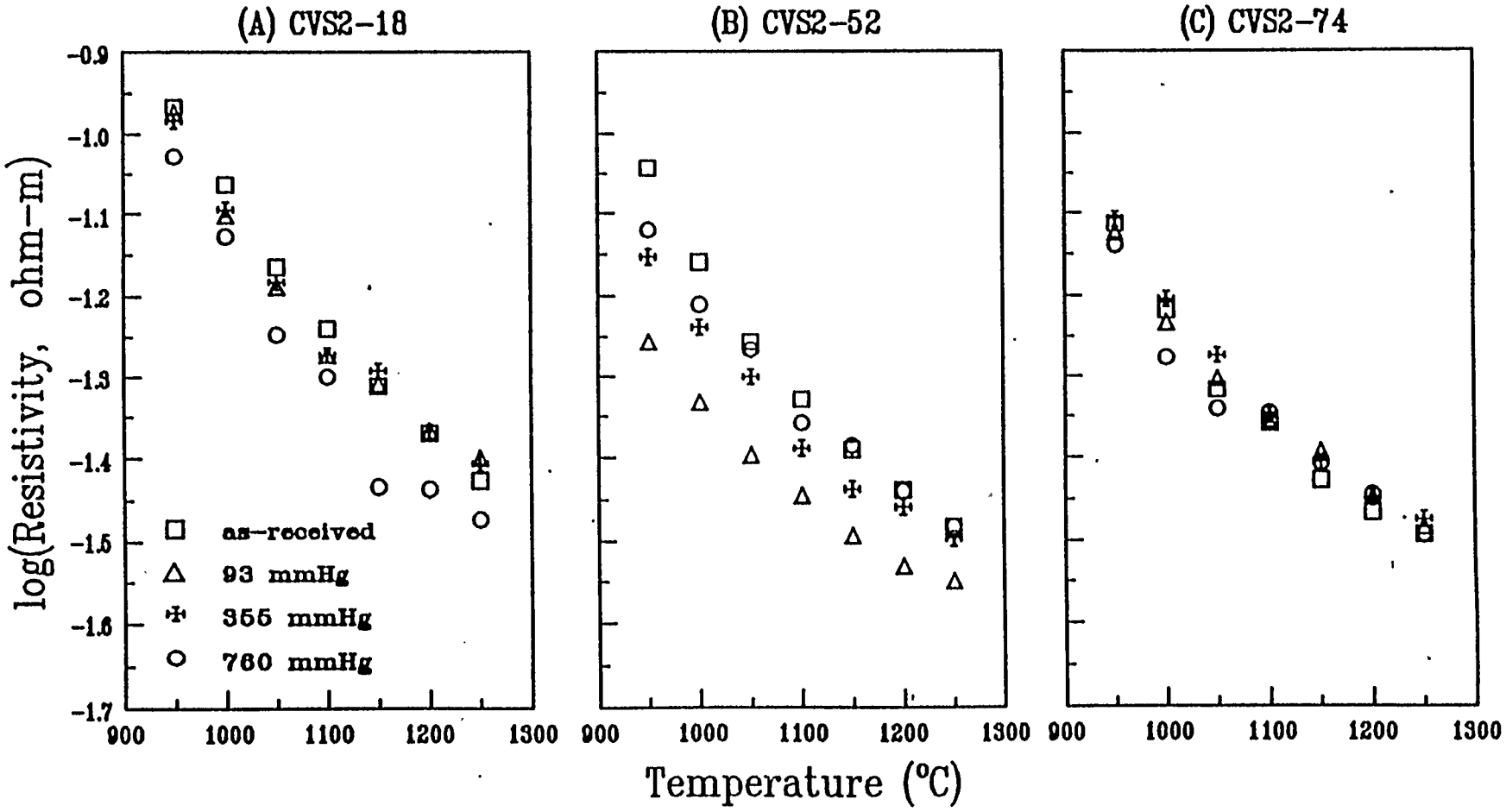

Figure 24 Electrical conductivity versus water concentration at 1150℃.

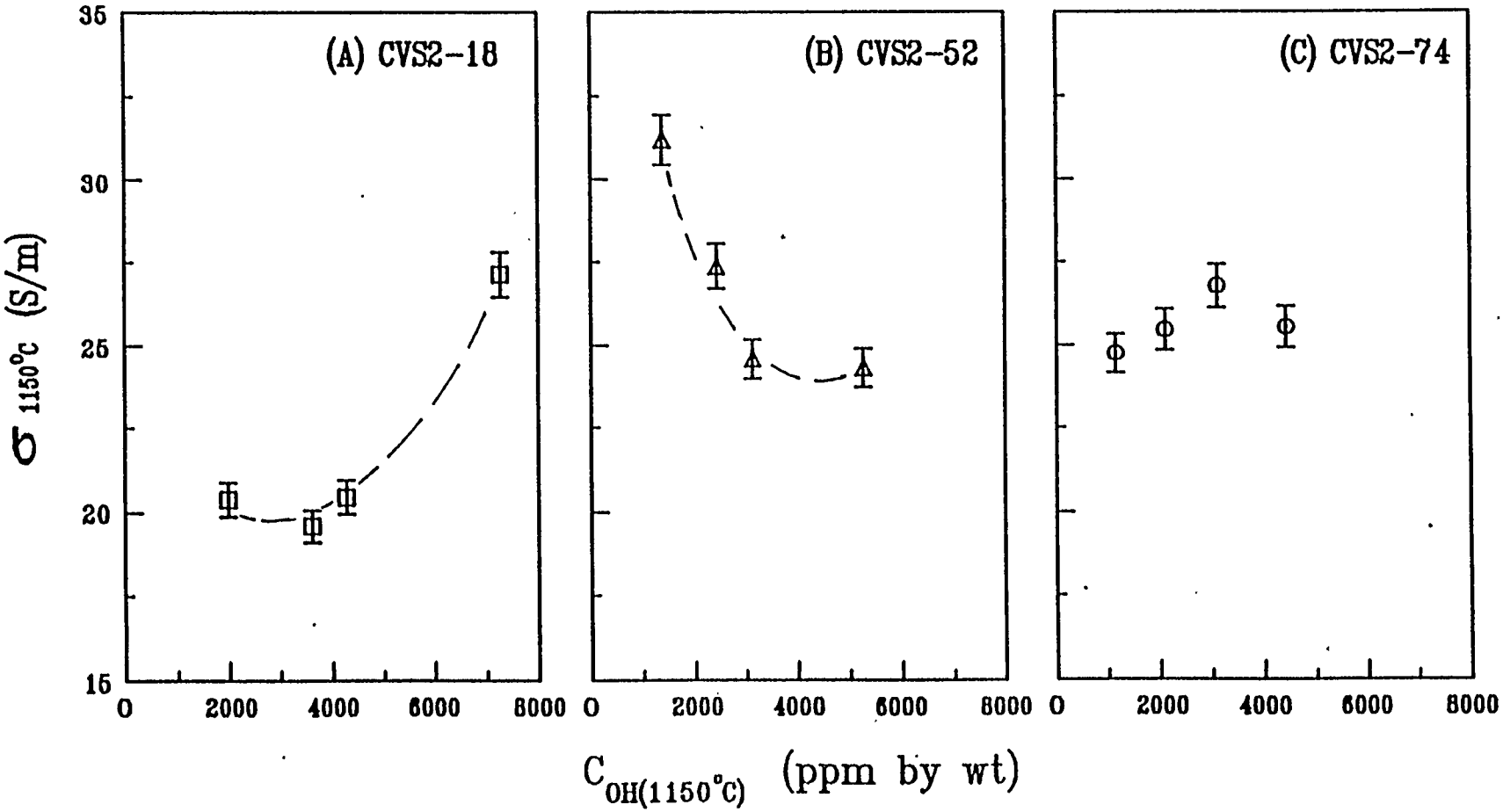

Figure 25 Comparison of pH values between the PCT and the MCC-1 tests for the simulated nuclear waste glasses.

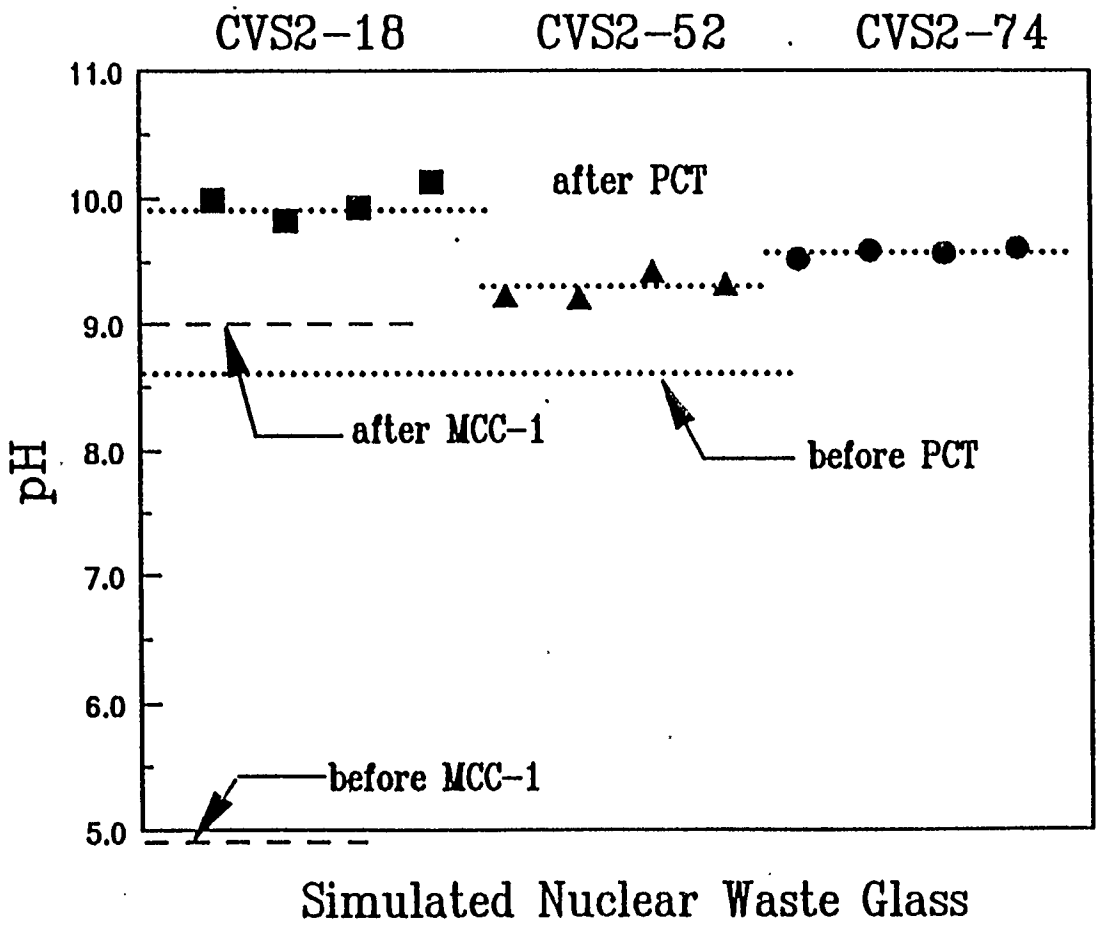

Figure 26 pH change as a function of time for the PCT and the MCC-1 tests.

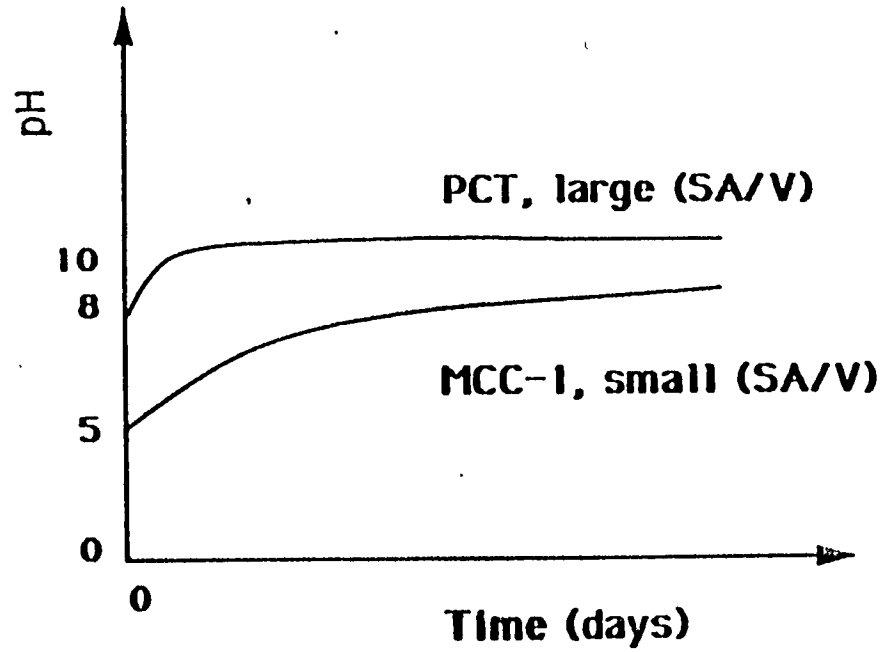

Figure 27 Different characteristics between the PCT and the MCC-1 tests in terms of pH, leached layer and dissolution processes for the simulated nuclear waste glasses.

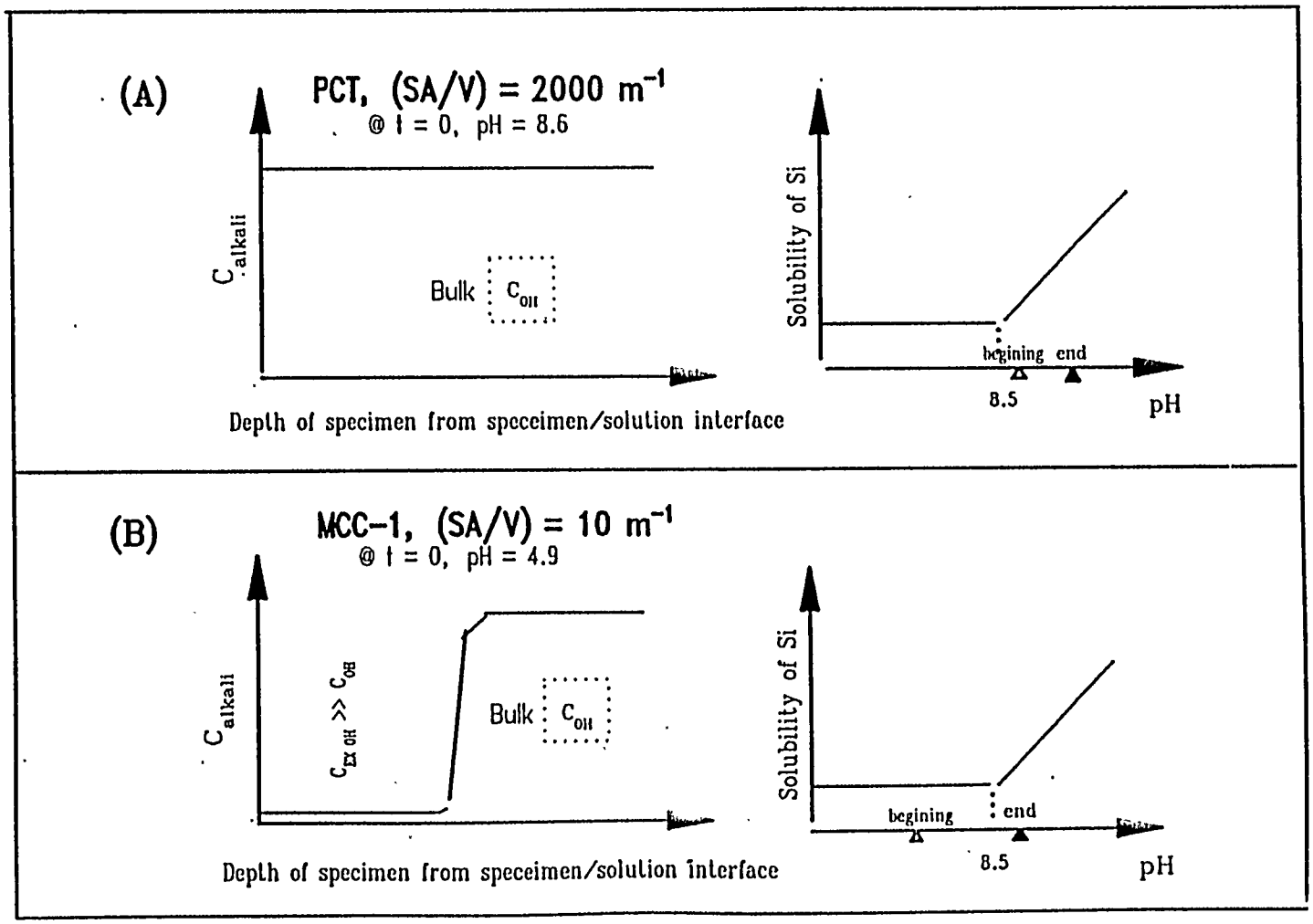

Figure 28 IR spectra of the CVS2-18 sample before and after the MCC-1 test indicating the OH change of both hydration and dehydration.

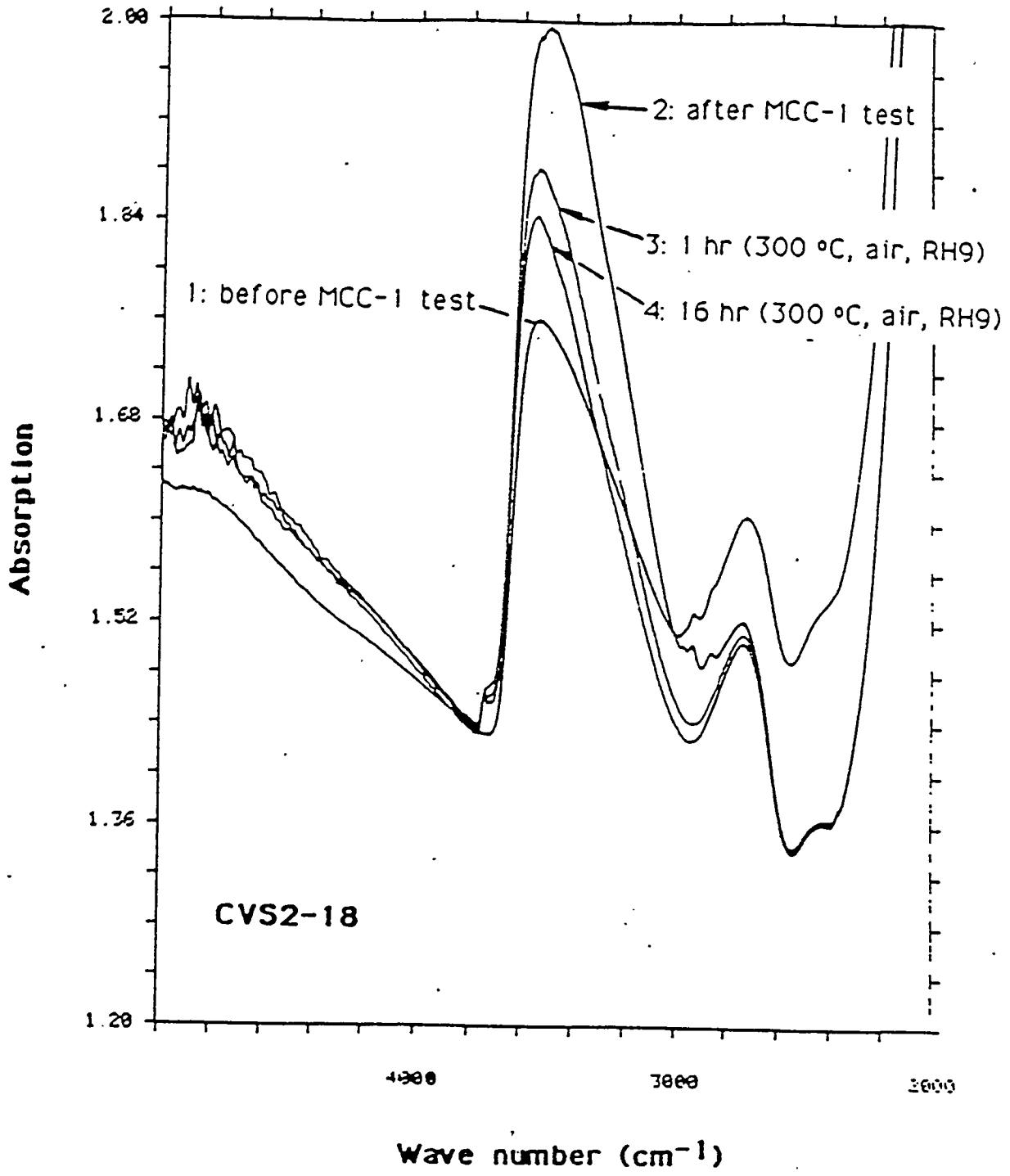

Figure 29 Comparison of experimental data with the results obtained by using Fulcher equation $\log\eta = A+B/(T(°C)-T_o)$.

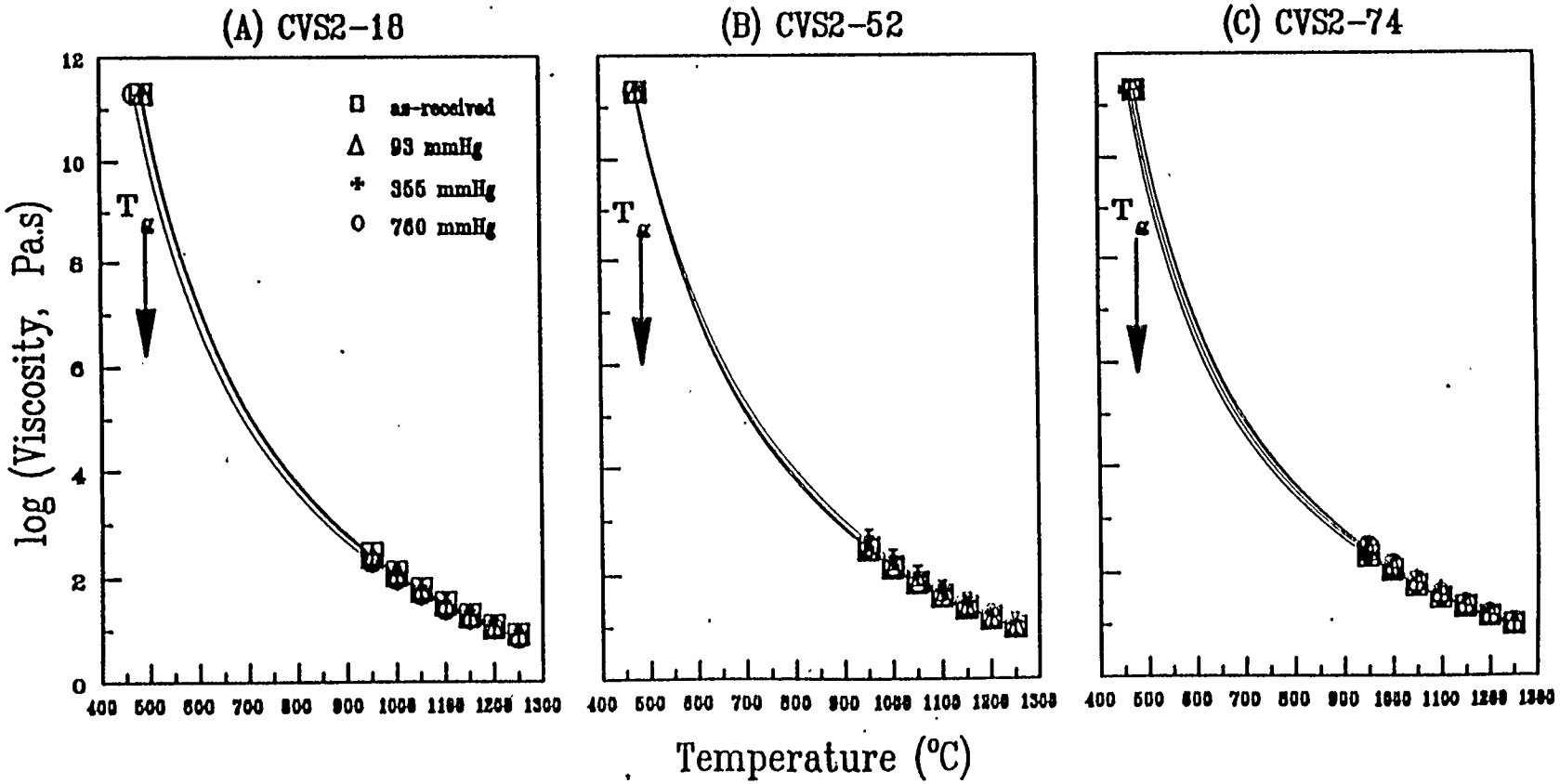

Figure 30 DC conductivity in $Na_2O.3SiO_2$ glass as a function of water content [29, 30].

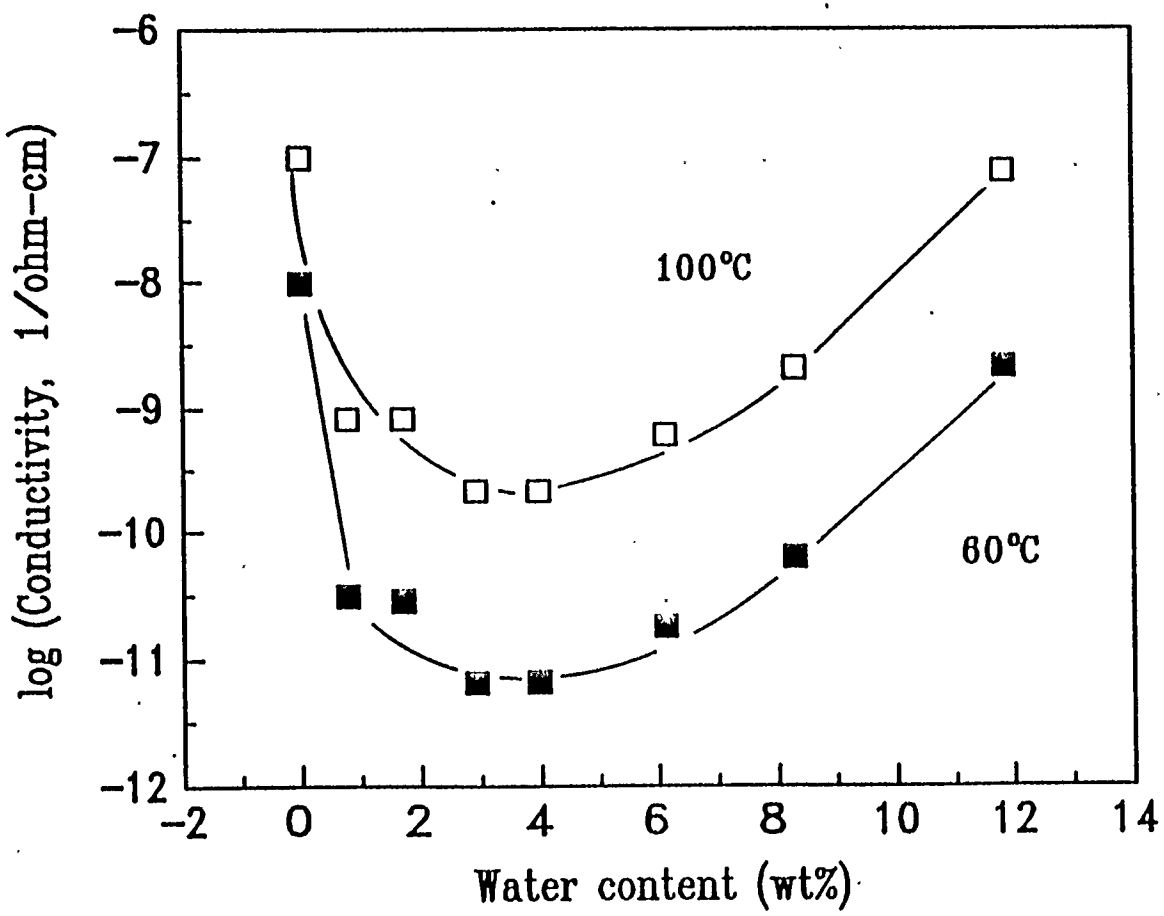

Figure 31 DC conductivity of $0.25[XK_2O+(1-X)Na_2O]-0.75SiO_2$ glass, showing mixed alkali effect at various temperatures [30].

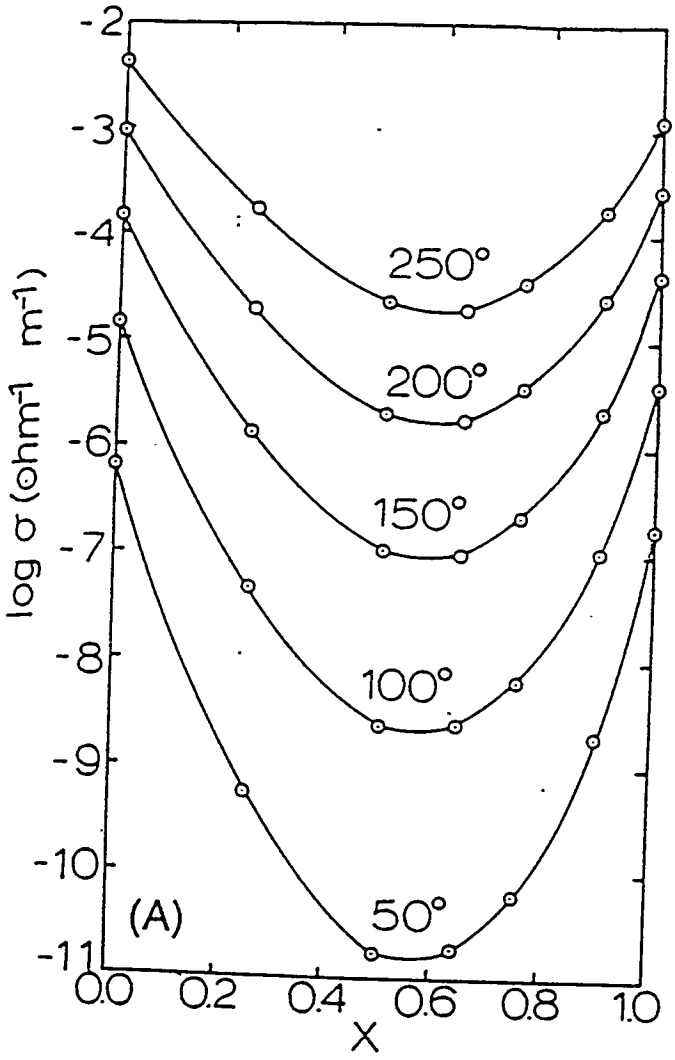

Figure 32 Comparison of experimental data with the results obtained by using Fulcher equation $\log\rho = A'+B'/(T(^{\circ}C)-T_o)$.

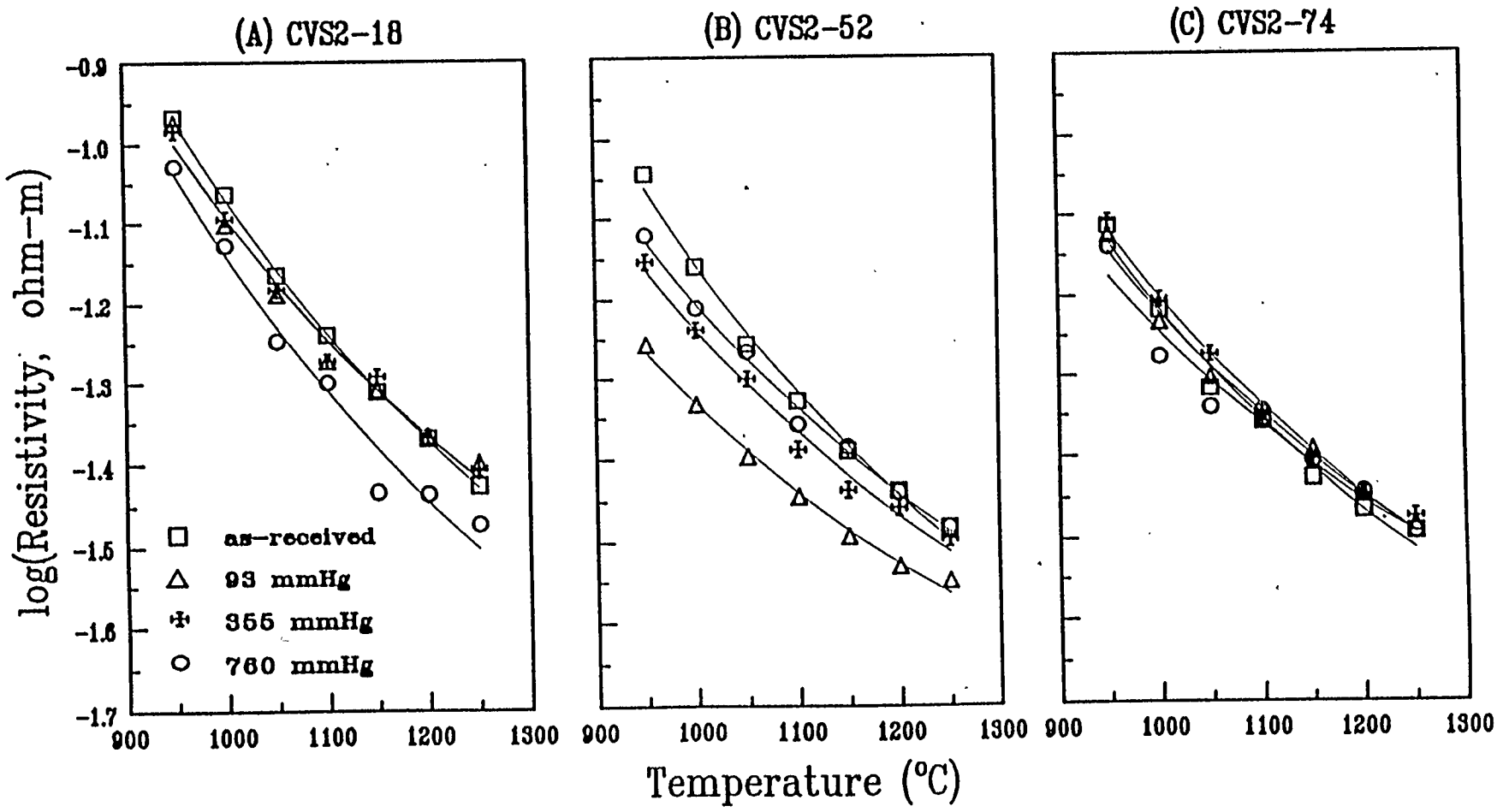

Appendix A1 Concentrations of Elements in the Leachate for the Simulated Nuclear Waste Glasses Tested using the MCC-1 Method (SA/V) = 10 m^{-1}, 28 days in type I water at 90 °C)

Element	Silicon (ppm)	Boron (ppm)	Lithium (ppm)	Sodium (ppm)
CVS2-18				
as-received	25.2±1.9	4.3±0.4	2.6±0.1	13.3±0.9
93 mmHg @	22.8±2.3	4.0±0.6	2.5±0.1	12.9±1.5
355 mmHg @	24.1±0.4	4.1±0.2	2.6± <0.1	13.7±0.4
760 mmHg @	19.8±1.9	3.9±0.2	2.5± <0.1	13.4±0.5
CVS2-52				
as-received	13.0±0.8	1.6±0.1	2.7±0.1	3.9±0.6
93 mmHg @	14.6± <0.1	1.3±0.3	2.8±0.1	3.5± <0.1
355 mmHg @	12.1±1.9	1.6±0.1	2.6±0.2	3.2±0.6
760 mmHg @	12.1±0.5	1.3±0.1	2.8±0.1	3.5±0.2
CVS2-74				
as-received	8.1($)	1.3($)	2.7($)	4.2($)
93 mmHg @	7.8±0.5	1.2±0.2	2.5± <0.1	4.7±0.3
355 mmHg @	6.7±1.0	1.0±0.3	2.4±0.1	4.3±0.6
760 mmHg @	6.9±0.2	1.0±0.1	2.5± <0.1	4.7±0.2

@ The value represents the saturated water vapor pressure under which these glasses were remelted.
($) A single value was used since other two sample leachates showed significantly lower pH values after the MCC-1.

Appendix A2 Normalized Elemental Mass Loss and pH Value for the Simulated Nuclear Waste Glasses (MCC-1 Test: (SA/V) = 10 m^{-1}, 28 days in type I water at 90 °C)

Element	Silicon (g/m^2)	Boron (g/m^2)	Lithium (g/m^2)	Sodium (g/m^2)	pH
CVS2-18					
as-received	10.1±0.8	13.2±1.1	15.2±0.5	15.9±1.1	8.95±0.05
93 mmHg @	9.1±0.9	12.2±1.7	14.6±0.7	15.4±1.8	8.95±0.10
355 mmHg @	9.6±0.2	12.6±0.5	14.9±0.1	16.4±0.5	8.91±0.04
760 mmHg @	7.9±0.8	11.9±0.5	14.6±0.2	16.1±0.5	8.88±0.01
CVS2-52					
as-received	4.7±0.3	6.2±0.5	7.4±0.2	11.6±1.8	8.89±0.03
93 mmHg @	5.2± <0.1	5.0±1.1	7.7±0.2	10.4±0.1	9.01±0.02
355 mmHg @	4.3±0.7	6.1±0.5	7.2±0.5	9.4±1.8	8.87±0.07
760 mmHg @	4.3±0.2	5.1±0.4	7.6±0.2	10.5±0.5	9.00±0.05
CVS2-74					
as-received	3.0 (#)	5.4 (#)	8.2 (#)	8.6 (#)	8.97 (#)
93 mmHg @	2.9±0.2	5.1±0.6	7.5±0.1	9.5±0.7	9.08±0.02
355 mmHg @	2.5±0.4	4.0±1.1	7.3±0.4	8.7±1.2	9.03±0.11
760 mmHg @	2.6±0.1	4.1±0.2	7.5±0.1	9.5±0.4	9.07±0.04

@ The value represents the saturated water vapor pressure under which these glasses were remelted.
(#) A single value was used since other two sample leachates showed significant lower pH values after the MCC-1 test (cf. Section 3.2).

Appendix B1 Concentrations of Elements in the Leachate for the Simulated Nuclear Waste Glasses Tested using the PCT Method (SA/V) = 2000 m^{-1}#, 7 days in type I water at 90 °C)

Element	Silicon (ppm)	Boron (ppm)	Lithium (ppm)	Sodium (ppm)
CVS2-18				
as-received	255.2±0.9	199.8±0.2	125.1±0.4	426.9±3.6
93 mmHg @	255.6±0.8	207.5±0.6	128.1±0.1	430.2±1.6
355 mmHg @	267.4±3.3	214.0±1.0	133.1±0.1	436.3±1.3
760 mmHg @	275.6±1.4	220.2±1.2	138.4±0.7	478.1±3.1
CVS2-52				
as-received	178.4±0.9	38.7±0.2	67.2±0.5	23.9±0.7
93 mmHg @	164.5±0.7	38.7±0.4	60.9±0.5	26.6±0.5
355 mmHg @	167.4±0.9	40.9±0.2	66.2±0.2	28.6±0.5
760 mmHg @	171.0±0.6	43.8±0.4	68.0±0.1	29.2±0.1
CVS2-74				
as-received	75.5±0.5	10.1±<0.1	24.1±0.2	14.5±0.1
93 mmHg @	81.2±<0.1	10.9±<0.1	26.6±0.1	14.8±0.2
355 mmHg @	89.7±0.5	12.9±0.2	29.5±0.1	14.9±0.1
760 mmHg @	103.0±0.3	15.0±0.1	37.6±0.3	19.9±0.4

The glass powder was collected using seives with 200 and 100 mesh, the particle size of which ranges from 75 μm to 150 μm.
@ The value represents the saturated water vapor pressure under which these glasses were remelted.

Appendix B2 - Normalized Elemental Mass Loss of Elements for the Simulated Nuclear Waste Glasses (PCT : (SA/V) = 2 mm^{-1}#, 7 days in type I water at 90 °C)

Element	Silicon (g/m^2)	Boron (g/m^2)	Lithium (g/m^2)	Sodium (g/m^2)
CVS2-18'				
as-received	0.51± <0.01	3.06± <0.01	3.60±0.01	2.56±0.02
93 mmHg @	0.51± <0.01	3.17±0.01	3.68± <0.01	2.58±0.01
355 mmHg @	0.53±0.01	3.27±0.02	3.83± <0.01	2.61±0.01
760 mmHg @	0.55± <0.01	3.37±0.02	3.98±0.02	2.86±0.02
CVS2-52				
as-received	0.32± <0.01	0.76±0.01	0.92±0.01	0.36±0.01
93 mmHg @	0.29± <0.01	0.76±0.01	0.83±0.01	0.40±0.01
355 mmHg @	0.30± <0.01	0.81± <0.01	0.91± <0.01	0.43±0.01
760 mmHg @	0.31± <0.01	0.86±0.01	0.93± <0.01	0.44± <0.01
CVS2-74				
as-received	0.14±0.01	0.21± <0.01	0.36± <0.01	0.15± <0.01
93 mmHg @	0.15± <0.01	0.23± <0.01	0.40± <0.01	0.15±0.01
355 mmHg @	0.17±0.01	0.27± <0.01	0.45± <0.01	0.15± <0.01
760 mmHg @	0.20± <0.01	0.31± <0.01	0.57± <0.01	0.20±0.01

(#) The glass powder was collected using seives with 200 and 100 mesh, the particle size of which ranges from 75 μm to 150 μm.
@ The value represents the saturated water vapor pressure under which these glasses were remelted.

Appendix B3 pH Value in Leachate for the Simulated Nuclear Waste Glasses Tested by the PCT Method. *

Sample	before	after
CVS2-18		
as-received	8.61	9.93
93 mmHg @	8.65	9.99
355 mmHg @	8.69	9.83
760 mmHg @	8.61	10.13
CVS2-52		
as-received	8.56	9.42
93 mmHg @	8.57	9.23
355 mmHg @	8.56	9.21
760 mmHg @	8.55	9.32
CVS2-74		
as-received	8.53	9.52
93 mmHg @	8.54	9.59
355 mmHg @	8.52	9.57
760 mmHg @	8.53	9.61

* pH values of the leachates were measured at room temperature.
@ The value represents the saturated water vapor pressure under which these glasses were remelted.

Appendix C1 Viscosity as a Function of Temperature for the Simulated Nuclear Waste Glasses (measured under different water vapor pressures)

Units: Pa.s

Temp (°C)	950	1000	1050	1100	1150	1200	1250
CVS2-18							
as-received	283.5	125.4	61.8	33.2	19.5	12.3	8.2
93 mmHg@	239.0	107.8	54.4	29.8	17.5	10.6	7.9
355 mmHg@	274.2	105.5	58.6	30.0	18.8	11.9	8.0
760 mmHg@	199.2	93.7	47.3	24.6	16.2	10.4	6.9
CVS2-52							
as-received	304.6	141.8	72.2	41.8	25.3	15.8	10.1
93 mmHg@	292.9	135.9	74.5	38.9	23.0	14.3	9.7
355 mmHg@	433.5	188.6	94.9	50.2	29.2	17.2	11.8
760 mmHg@	349.2	147.6	72.2	38.7	23.9	14.8	9.5
CVS2-74							
as-received	194.5	104.3	54.4	32.1	21.8	14.4	10.1
93 mmHg@	247.5	126.5	67.0	41.8	24.6	16.1	10.7
355 mmHg@	229.7	112.5	60.9	36.2	22.5	15.0	10.6
760 mmHg@	278.9	130.1	63.7	36.1	23.7	14.9	10.5

@ The values are the saturated water vapor pressures under which the glasses were remelted and the viscosities were measured.

Appendix C2 Regression Analysis of Viscosity as a Function of Temperature using Fulcher Equation: $\log\eta = A + B/[T(°C) - T_o]$ for the Simulated Nuclear Waste Glasses#

Fitting Parameter	A (log (Pa.s))	B (°C)	T_o (°C)
CVS2-18			
as-received	-2.93±0.07	3995.4±84.2	205.2±4.5
93 mmHg@	-2.78±0.10	3744.7±116.4	222.1±6.4
355 mmHg@	-2.85±0.16	3879.0±179.9	209.8±9.8
760 mmHg@	-2.83±0.11	3833.5±124.7	199.6±6.8
CVS2-52			
as-received	-2.65±0.08	3843.4±98.3	200.5±5.2
93 mmHg@	-2.77±0.06	3954.7±68.9	195.0±3.8
355 mmHg@	-3.06±0.08	4456.6±93.3	165.6±4.9
760 mmHg@	-3.06±0.13	4344.0±139.5	170.6±7.4
CVS2-74			
as-received	-2.14±0.07	3222.6±78.0	221.2±4.7
93 mmHg@	-2.25±0.04	3372.7±55.6	225.2±3.2
355 mmHg@	-2.25±0.05	3356.8±57.8	219.2±3.3
760 mmHg@	-2.52±0.12	3655.5±136.9	209.4±7.7

In the analyses, the viscosity of $10^{11.3}$ Pa.s at the glass transition temperature, T_g, determined by DSC method, was used for all glasses.
@ The values are the saturated water vapor pressures under which the glasses were remelted and the viscosities were measured.

Appendix D1 Electrical Conductivity as a Function of Temperature for the Simulated Nuclear Waste Glasses (measured under different water vapor pressures)

Units: S/m

Temp (°C)	950	1000	1050	1100	1150	1200	1250
CVS2-18							
as-received	9.27	11.57	14.61	17.35	20.46	23.42	26.69
93 mmHg@	9.41	12.66	15.44	18.73	20.38	23.27	25.14
355 mmHg@	9.63	12.44	15.24	18.73	19.60	23.36	25.50
760 mmHg@	10.68	13.43	17.65	19.93	27.13	27.32	29.74
CVS2-52							
as-received	11.05	14.43	18.04	21.31	24.59	27.47	30.40
93 mmHg@	18.03	21.50	24.94	27.87	31.19	34.00	35.44
355 mmHg@	14.23	17.29	19.97	24.49	27.38	28.79	31.41
760 mmHg@	13.21	16.24	18.46	22.81	24.31	27.58	30.41
CVS2-74							
as-received	12.97	16.54	20.76	22.67	26.77	29.25	31.15
93 mmHg@	13.32	17.10	20.12	22.84	24.75	28.05	30.49
355 mmHg@	12.81	16.01	18.80	22.39	25.47	28.06	29.85
760 mmHg@	13.79	18.90	21.93	22.18	25.54	27.81	31.17

@ The values are saturated water vapor pressure under which the samples were remelted at 1150 °C and the electrical conductivities were measured.

Appendix D2 Regression Analysis of Electrical Resistivity as a Function of Temperature using Fulcher Equation: $\log\rho = A' + B'/[T(°C) - T_o]$ for the Simulated Nuclear Waste Glasses

Fitting Parameter	A' (log (ohm-m))	B' (°C)	T_o (°C) $
CVS2-18			
as-received	-2.58±0.02	1196.8±13.2	205.2
93 mmHg@	-2.44±0.07	1050.1±58.2	222.1
355 mmHg@	-2.45±0.06	1073.4±51.9	209.8
760 mmHg@	-2.67±0.10	1222.2±124.7	199.6
CVS2-52			
as-received	-2.59±0.05	1146.8±42.5	200.5
93 mmHg@	-2.32±0.03	793.7±30.3	195.0
355 mmHg@	-2.43±0.06	993.0±51.9	165.6
760 mmHg@	-2.42±0.04	1010.2±36.8	170.6
CVS2-74			
as-received	-2.44±0.06	952.0±52.5	221.2
93 mmHg@	-2.33±0.05	860.7±39.9	225.2
355 mmHg@	-2.40±0.04	939.3±34.6	219.2
760 mmHg@	-2.28±0.09	819.0±80.2	209.4

@ The values are the saturated water vapor pressures under which the glasses were remelted and the resistivities were measured.
$ T_o values were taken from data obtained by using the Fulcher analyses of the viscosity data for each identical sample melt condition.